University of Texas at El Paso
DigitalCommons@UTEP

Open Access Theses & Dissertations

2017-01-01

4-Nonylphenol Induces Neurodegeneration By Altering Cytoskeleton

Cynthia Carreon
University of Texas at El Paso, tesakam08@gmail.com

Follow this and additional works at: https://digitalcommons.utep.edu/open_etd


Part of the Biology Commons, Cell Biology Commons, and the Neuroscience and Neurobiology Commons

Recommended Citation
Carreon, Cynthia, "4-Nonylphenol Induces Neurodegeneration By Altering Cytoskeleton" (2017). *Open Access Theses & Dissertations*. 420.
https://digitalcommons.utep.edu/open_etd/420

This is brought to you for free and open access by DigitalCommons@UTEP. It has been accepted for inclusion in Open Access Theses & Dissertations by an authorized administrator of DigitalCommons@UTEP. For more information, please contact lweber@utep.edu.

4-NONYLPHENOL INDUCES NEURODEGENERATION BY ALTERING CYTOSKELETON

CYNTHIA CARREON

Master's Program in Biological Sciences

APPROVED:

Sukla Roychowdhury, Ph.D., Chair

Igor Almeida, Ph.D.

Binata Joddar, Ph.D.

Kristine Garza, Ph.D.

Manuel Miranda, Ph.D.

Charles Ambler, Ph.D.
Dean of the Graduate School

4-NONYLPHENOL INDUCES NEURODEGENERATION BY ALTERING CYTOSKELETON

By

CYNTHIA CARREON, B.S.

THESIS

Presented to the Faculty of the Graduate School of

The University of Texas at El Paso

in Partial Fulfillment

of the Requirements

for the Degree of

MASTER OF SCIENCE

Department of Biological Sciences

THE UNIVERSITY OF TEXAS AT EL PASO

December 2017

ACKNOWLEDGEMENTS

This was an incredible journey that would not have been the same without the help of many people. My committee members, Dr. Garza, Dr. Joddar, Dr. Miranda, and Dr. Almeida were outstanding in guiding me throughout the whole project. I would like to acknowledge Dr. Almeida and Marcela Aguilera-Flores for helping me with their expertise in proteomic analysis. Without the help of these individuals I would not have been able to accomplish a major research project such as this.

I am grateful for my mentor, Dr. Sukla Roychowdhury, whose patience and assistance helped me to complete the research experiments that were needed to put the topic together. Of course, this project would not have been possible without the participation of others including Dr. Jorge Sierra-Fonseca and Amaris Castañón whom I sincerely thank for their advice and willingness to help me. For many memorable days, I must thank my lab mates, Luisa Sanchez and Clarissa Palacios, without them the lab would've been lonely and uncomfortably quiet. I must also thank my former lab mates Myriah Acuña and Alexa Montoya for the stimulating discussions and working together before deadlines.

Even though they were not in the lab with me, I would like to give my thanks and appreciation to my parents for their unfailing support and continuous encouragement throughout my years of study and through the process of researching and in writing this thesis. Finally, and just as important, my significant other Sal Solis for always being there for me; in the late nights, and vacations full of work. Thank you.

ABSTRACT

4-nonylphenol (4-NP), an endocrine-disrupting compound (EDC), has been shown to affect brain development and may cause neurodegeneration. In the environment, 4-NP arises as a degradation product of alkylphenol polyethoxylates, compounds widely used as nonionic surfactants in commercial production, as well as in herbicides, pesticides, polystyrene plastics, and paints and has been shown to undergo a high level of accumulation in biological tissues. However, the mechanism by which 4-NP exerts its effect is not understood. Recent results from our laboratory indicate that Gβγ, an important component of the G protein-signaling pathway, induces neuronal outgrowth and differentiation by modulating microtubule (MT) assembly, and 4-NP interferes with this process. 4-NP has been shown to inhibit neurotrophin-dependent neurite formation and cellular aggregation in cultured PC12 cells. 4-NP also inhibited neurite outgrowth of Gβγ-overexpressed PC12 cells. Based on these results, I *hypothesize that 4-NP inhibits neurite outgrowth and induces neurodegeneration by disrupting MTs and associated proteins through Gβγ mediated pathway.* PC12 cells were used for this study because they respond to nerve growth factor (NGF) and exhibit a typical phenotype of neurons. In Specific Aim 1, using biochemical, pharmacological, and immunoconfocal methodologies, I have demonstrated that 4-NP inhibited tubulin expression, disrupted polymer-monomer equilibrium and MT organization, and inhibited MT-Gβγ interactions in NGF-differentiated PC12 cells. In Specific Aim 2, I have conducted the proteomic analysis of 4-NP treated cells and found that the compound affected the cytoskeletal profile in NGF-differentiated PC12 cells. Principle Component analysis (PCA) using Scaffold-Perspective software showed that 4-NP significantly affected the protein composition/pattern of CSK in NGF-differentiated PC12 cells. In summary, I concluded that one of the mechanisms by

which 4-NP causes neuronal damage is by altering the Gβγ- cytoskeletal mediated pathway, which is critical for neuronal growth and development.

TABLE OF CONTENTS

LIST OF FIGURES

LIST OF TABLES

CHAPTER I: INTRODUCTION

1.1. 4-Nolylphenol (4-NP)

Endocrine disrupting compounds (EDC's) have been found in foods, pesticides, industrial chemicals, and consumer products and there are increasing concerns about the potential hazards they pose for our health. These compounds ~~also~~ play a role in disturbing homeostatic control and contribute to psychological disorders, cancer, and defects in reproductive, behavioral, and immune functions (Safe, 2000). 4-nonylphenol (4-NP), an endocrine-disrupting compound (EDC), has been shown to affect brain development and may cause neurodegeneration (California Environmental Protection Agency, 2009). 4-NP is a synthetic organic chemical produced in relatively large quantities in the U.S. and used primarily in making detergents, pesticides, plastics, and rubber, as well as other commercial uses. Human exposure to 4-NP may occur through ingestion of contaminated foods, drinking water, and contact with detergents. In the environment, 4-NP arises as a degradation product of alkylphenol polyethoxylates, compounds widely used as nonionic surfactants in commercial production of industrial cleaners as well as in agricultural pesticides, polystyrene, plastics, and paint production and has been shown to undergo a high level of accumulation in biological tissues (U.S. Environmental Agency, 2010) (**Fig. 1.1**). Tissue concentration of 4-NP has been measured in the 1-20□M range in aquatic organisms (Bevan, 2006). Human exposure to 4-NP may occur through ingestion of contaminated foods, drinking water, and contact with detergents. Because of its potential environmental toxicity issues, European countries have restricted or banned the use of NPEO since 1980s (Renner, 1997). Because toxicity and risk at low concentrations have not been clearly proven, United States allowed its use. However, the level of risk to humans and the environment posed by 4-NP is currently under considerable debate by researchers, chemical manufacturers, and regulators.

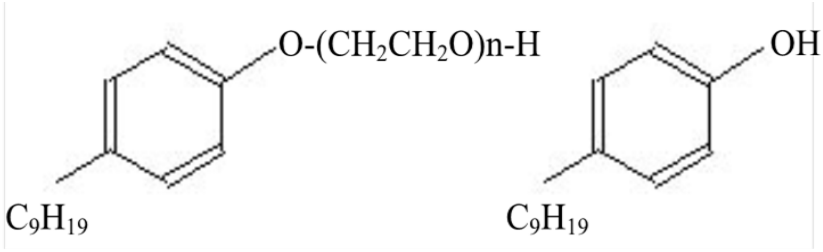

Nonylphenol polyethoxylate (NPE) Nonylphenol (NP)

[**Fig. 1.1. Chemical structures of nonylphenol polyethoxylate and nonylphenol**]

1.2 4-Nolylphenol (4-NP) and Neurodegeneration.

4-NP, along with other EDCs, have been shown to induce deterioration of neural development, decrease memory and learning capacity and spatial learning in monkey and rat offspring born from mothers exposed to EDCs (Yoshikawa, 2005). Other studies have exhibited that gestational 4-NP exposure produced a significant decrease in credits in learning and memory functions of offspring rats (Xu et. al 2010). These data indicate that 4-NP exposure may have potentially damaging effect during early neuronal development. 4-NP has been shown to induce the death of neural stem cells suggesting that 4-NP might directly cause neurodegeneration (Kudo et al, 2004).

Neurodegeneration is a pathological condition associated with the progressive loss of neurons which occurs in many neurological disorders including Alzheimer's disease, Parkinson's disease, and schizophrenia. However, the cause of neurodegenerative disorders is unknown and there are currently no effective drugs available to treat the disease processes. Cytoskeletal disruption in neurons and aggregation of proteins associated with these diseases is the hallmark of neurodegeneration (Alonzo, 2008; Amniai, 2008; Gustav-rothenberg, 2010). Aging is the most consistent risk factor for developing a neurodegenerative disorder, and recent evidence suggests that environmental factors, which act as endocrine disruptors, pose a risk in the disease process.

More recently, 4-NP has been shown to inhibit neurotrophin-dependent neurite outgrowth in cultured embryonic *Xenopus* spinal-cord neurons and PC12 cells. Interestingly, the effect of 4-NP was not inhibited by the nuclear estrogen receptor antagonist, ICI182,780, but was inhibited by the G protein antagonist, pertussis toxin (Bevan, 2006) suggesting a role of G protein signaling in this process.

1.3 Neuronal Cytoskeleton, Neurite Outgrowth, and Neurodegeneration

Neurite outgrowth and differentiation is a complex process in which two distinct domains emerge from the cell body: a long, thin axon that transmits signals and multiple shorter dendrites that are specialized to receive signals (Sierra-Fonseca, 2014). When fully differentiated through elongation of axon and dendrites, this morphology allows neurons to achieve precise connectivity between appropriate sets of neurons, which is fundamental to the proper functioning of the nervous system. Assembly and disassembly of the cytoskeleton is critical for axon and dendrite formation as well as for neurite outgrowth. MTs and actin filaments are two major protein filaments that constitute the neuronal cytoskeleton. MTs form dense parallel arrays in axons and dendrites that are required for the growth and maintenance of these neurites (Witte and Bradke; Geraldo and Gordon-Weeks, 2009) (**Fig. 2.1**). Unlike MTs, actin filaments in neurons are enriched in the growth cone and organized into long bundles forming filamentous protrusions (filopodia) or veil-like sheets of branched actin (lamellipodia) (Witte, 2008; Geraldo, 2009). Selective stabilization of MTs also occurs during neuronal differentiation (Bulinsky and Gundersen, 1991).

During neurodegeneration, the MT assembly and proteins associated with them are severely altered. In Alzheimer's disease, amyloid plaques and neurofibrillary tangles (NFT) comprise the two major neuropathologic brain alterations. NFT are formed from paired helical filaments (PHF) consisting of tau, a microtubule-associated protein (MAP). Under normal conditions, tau binds to MT, stabilizing neuron structure and integrity. In an AD brain, the MT structure is disrupted, which causes tau to be hyperphosphorylated and not bind to the MTs (**Fig. 3.1**). Lewy bodies, which are considered cytopathological markers of Parkinson's disease (PD), are comprised of tubulins (subunit protein of MTs) MAP1, and MAP2 (Alonso et al., 2008; Amniai et al., 2008; Gustav et al., 2010). However, the mechanism by which diseases are triggered and

then progress is not well understood. Recent results suggest that MT assembly is severely compromised in both the AD and PD brains (Cash et al., 2003; Cartelli et al., 2010; Cartelli et al., 2013). This could play a significant role in triggering early disease. Recently, we have found that the interaction of Gβγ with MTs is important for nerve growth factor (NGF)-induced neuronal differentiation of PC12 cells and that the sequestration of Gβγ by GRK2i, a Gβγ-inhibitory peptide, inhibits neurite outgrowth and affects MT organization, thus indicating the important role of Gβγ in this process. Recent results from our laboratory indicate that Gβγ, an important component of the G protein-signaling pathway, induces neuronal outgrowth and differentiation by modulating microtubules (MT) assembly (Roychowdhury, 1997; Roychowdhury, 2006; Montoya, 2007; Sierra-Fonseca, 2014) (**Fig. 2.1**).

4-NP has been shown to inhibit neurotrophin-dependent neurite formation and cellular aggregation in cultured PC12 cells. 4-NP also inhibited neurite outgrowth of Gβγ-overexpressed PC12 cells and caused microtubule disruption, cellular aggregation and degeneration (Martinez J, UTEP MS thesis, 2013).

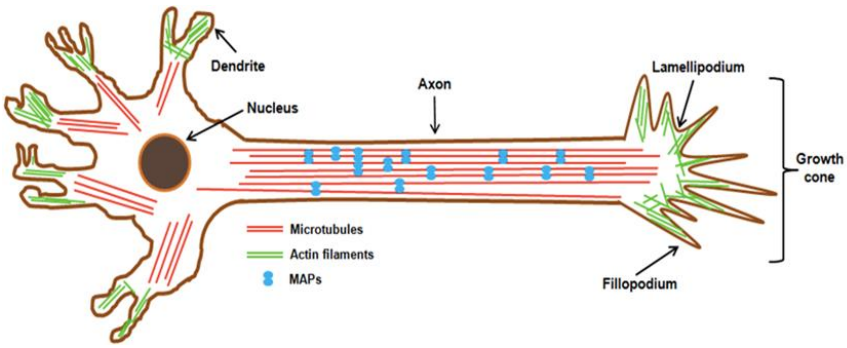

[**Fig. 2**.1 **Neuronal Cytoskeleton.**

In neuronal cells, MTs are found in the axon of the cell and in the dendrites (red filaments). Actin filaments (green) are present in the growth cone and the tips of the dendrites close to the plasma membrane, where they play a role in maintaining cell shape. MAPs (blue dots) are found in the axon where they participate in MT bundling.]

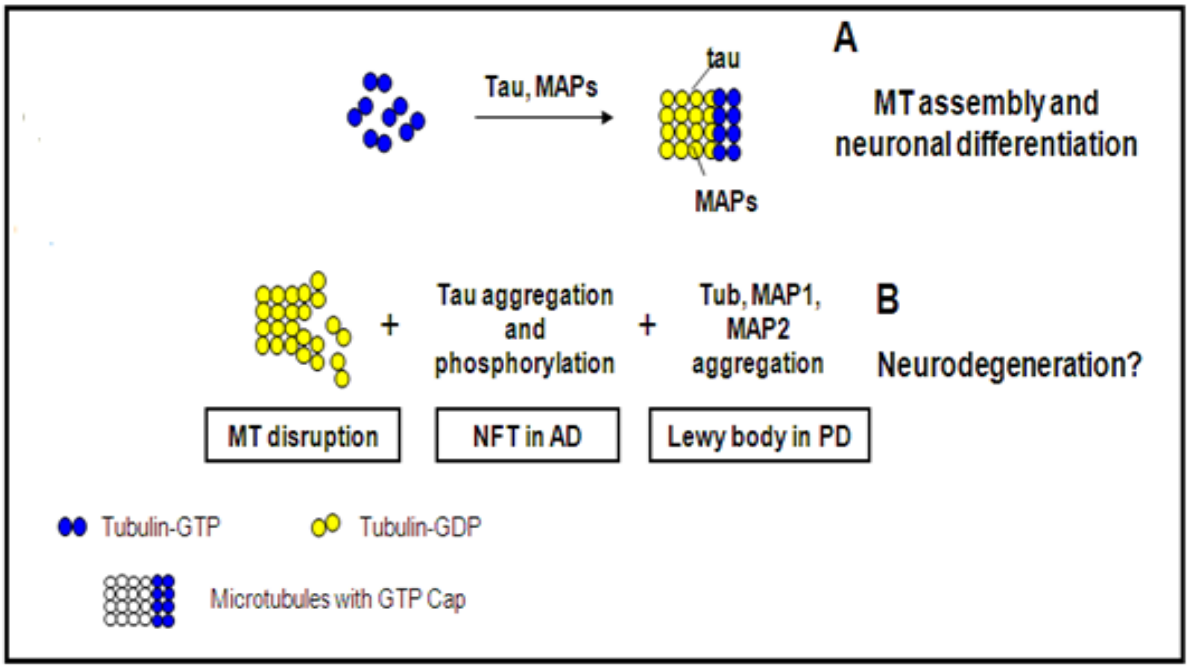

[**Figure 3.1 MT assembly and its possible role in neurodegeneration.**

Irregular organization of the MT cytoskeleton is known to be a feature of neurodegeneration in Alzheimer's disease (AD) and Parkinson's disease (PD). Since Gβγ is known to have a role in the regulation of MT assembly, we propose that blocking the interaction of Gβγ with tubulin/MTs by 4-NP will alter MT organization in neuronal cell models and ultimately lead to neurodegeneration.]

1.4 Microtubule (MT) Assembly and G protein-mediated signaling

G protein-mediated signaling is a major signaling pathway in neurons that consists of three components; G protein-coupled receptors (GPCRs), G protein, and effector molecules. GPCRs constitute the largest family of transmembrane receptors and mediate the action of extracellular signals as diverse as light, odorants, peptide hormones, and neurotransmitters. Current models of G proteins favor a heterotrimeric structure composed of the guanine- nucleotide binding α plus β and γ subunits, the latter two forming a tight association under nondenaturing conditions. Agonist-bound receptors activate G proteins by allowing GTP to bind to the βγ subunit of the heterotrimer. Subsequently, activated Gα changes its association with Gβγ in a manner that allows both subunits to contribute to the regulation of intracellular-effector molecules (Fig. 4.1). Results from our laboratory indicate that β and γ subunits of G proteins regulate microtubule assembly *in vitro* (Roychowdhury and Rasenick, 1997; Roychowdhury et al., 1999; Roychowdhury et al., 2006; Montoya et al., 2007). While Gβ activates tubulin GTPase and inhibits microtubule assembly, Gβγ promotes tubulin polymerization. Reconstituted heterotrimers were shown to be inactive in promoting microtubule assembly, which suggests that G-protein activation is necessary for the modulation of microtubules by G-protein subunits. Using the anti-mitotic agent nocodazole, it has been demonstrated that the tubulin-Gβγ interaction is important for MT assembly in cultured PC12 and NIH3T3 cells (Montoya et al., 2007). More recently, it was found that Gβγ–MT interaction is critical for NGF-induced neuronal differentiation of PC12 cells. Overexpression of Gβγ in PC12 cells (in the absence of NGF) induced neurite formation that is seen in NGF-differentiated cells. Altogether, results from our laboratory suggested that the Gβγ, initiated by the activation of the G protein-coupled receptor (GPCR), is a signal-transducing protein complex, and its interaction with

microtubules (MTs) is important to neuronal development, differentiation, structure, and neurodegeneration (Figure 4.1).

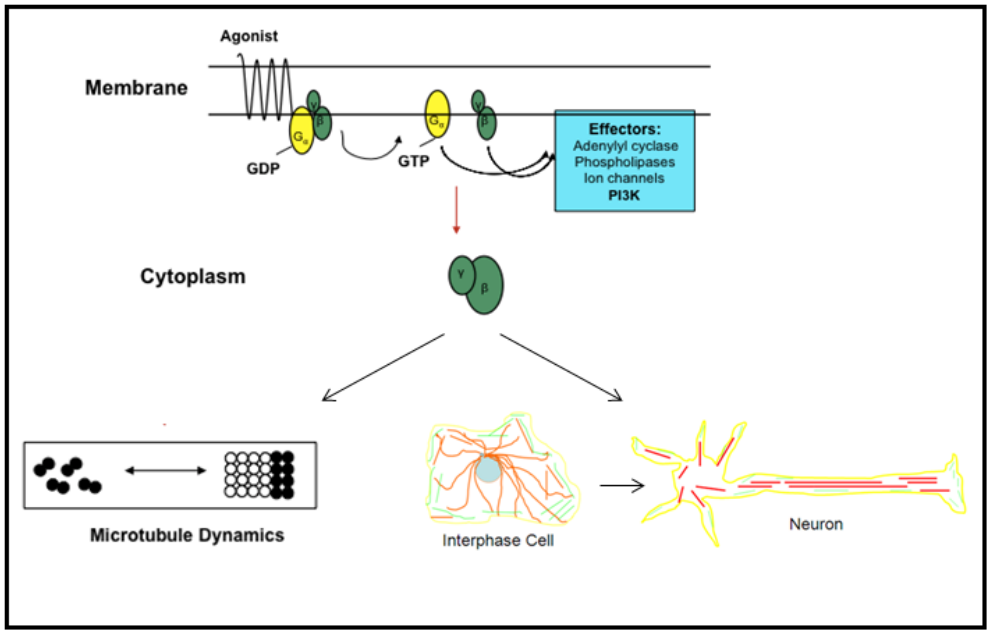

[**Fig. 4.1 Regulation of microtubule assembly and neurite outgrowth by Gβγ-mediated pathway.**

G-protein signaling is initiated when the seven-transmembrane domain G-protein coupled receptor (GPCR) is activated by an agonist. The Gαβγ Heterotrimer disassociates into Gα and Gβγ subunits, which are then free to activate different effector molecules. Gβγ interacts with MTs and promotes MT assembly.]

1.5 Proteomic analysis and Mass Spectrometry

Proteomics, the large-scale analysis of proteins, has been inspired by the realization that the final product of a gene is inherently more complex and closer to function than the gene itself (Graves, 2002). It is impossible to explain mechanisms of disease, aging, and effects of the environment solely by studying the genome. By studying proteins, protein post-translational modifications can be characterized and drug targets can be identified. Also, using proteomics protein-protein interaction can be identified making possible the discovery of the involvement of proteins in metabolic pathways.

There are multiple methods to perform proteomics analysis but the method of choice is mass spectrometry (MS). MS is an analytical technique that is used to identify and quantify unknown materials within a sample by ionizing chemical species and characterize the ions by their mass to charge ratio (m/z) and abundance. The mass spectrometer is the instrument used to perform MS analysis. Software like Protein Discoverer by Thermofisher is used to quantify proteins obtained from LC MS/MS. To do the statistical analysis Scaffold Proteome Software is used.

HYPOTHESIS AND SPECIFIC AIMS

The objective of my research is to understand the mechanism by which 4-NP, an endocrine disrupting compound (EDC) induces neurodegeneration. Results from our laboratory have shown the Gβγ, an important component of GPCR pathway is involved in neuronal differentiation (Sierra-Fonseca, 2014). It was found that the interaction of Gβγ with MTs is important for nerve growth factor (NGF)-induced neuronal differentiation of PC12 cells and that the sequestration of Gβγ by GRK2i, a Gβγ-inhibitory peptide, disrupted MTs, inhibited neurite outgrowth and induced neurite damage, thus indicating the important role of Gβγ in this process (Sierra-Fonseca 2014). Therefore, I hypothesize that 4-NP inhibits neurite outgrowth and induces neurodegeneration in PC12 cell model by disrupting MTs cytoskeleton through Gβγ mediated pathway. I plan to test the hypothesis by focusing on the following aims in this study:

Specific Aim 1: Determine if 4-nonylphenol alters MTs cytoskeleton through Gβγ mediated pathway.

Specific Aim 2: Examine the cytoskeletal disruption and neurodegeneration induced by 4-nonylphenol by proteomic analysis.

CHAPTER 2: MATERIALS AND METHODS

2.1.Cell Culture, NGF and 4-NP Treatment

PC12 cells (pheochromocytoma cells derived from the adrenal gland of *Rattus norvegicus*) were grown at 37 °C in 75-cm^2 culture flasks in Dulbecco's modified Eagle's Medium (DMEM) (4.5 g/L glucose, L-glutamine, without pyruvate), supplemented with 10% bovine calf serum (BCS) and antibiotics (100 U/mL penicillin, and 100 µg/mL streptomycin). For NGF treatment, PC12 cells were grown on 100- 150-mm plates to 70% confluence over 1–2 days, and then treated with 100 ng/ml of NGF (Sigma-Aldrich, St. Louis, MO) dissolved in complete media for 3 consecutive days. Control cells (without NGF treatment) were also grown under the same conditions. Cells were treated with 5µM or 10µM 4-Nonylphenol for 1 hour or overnight. A stock solution of 10 mM 4-NP was prepared in DMSO and diluted in DMEM media to a final concentration of 5 or 10 µM 4-NP and added to the cells as indicated in the figures.

2.2. Extraction of Cytoskeletal (CSK) and Soluble Protein (SOL) Fractions.

PC12 cells were grown in 100- or 150-mm plates to 70% confluence over 1–2 days and subjected to NGF treatment as described above. The plates were used in duplicates for each condition. Subsequently, the plates were treated with or without 4-NP for 1 hour or overnight. Cytoskeletal (CSK) and soluble (SOL) fractions were prepared by extracting soluble proteins in an MT-stabilizing buffer (MS). The stabilizing buffer contained 0.1 M PIPES, pH 6.9, 2 M glycerol, 5 mM $MgCl_2$, 2 mM EGTA, 0.5% Triton X-100, protease inhibitor cocktail (Sigma-Aldrich), 0.1 mM GTP, and 1 mM DTT. Briefly, cells were rinsed and incubated with MS buffer (0.5–1 ml) for ~10 minutes at room temperature until cells were beginning to lyse. Subsequently, cells were removed mechanically (using a cell scraper) and centrifuged at 10,000 × g for 10 min. The

supernatant constitutes the SOL fraction, and the cell pellets represent the CSK fraction. Cytoskeletal pellets were washed and resuspended in 0.25 mL PEM (0.1 M PIPES, pH 6.9, 0.5 mM $MgCl_2$, 1 mM EGTA) buffer, kept on ice for 15 min to depolymerize the MTs, sonicated on ice for 1 min, and clarified by centrifugation. The protein concentration of the samples was determined using the Bio-Rad protein assay, using bovine serum albumin (BSA) as a standard.

2.3. Preparation of Whole-cell lysate

PC12 cells were grown in 100-mm 150-mm plates to 80% confluence over 1-2 days, treated with or without NGF. Subsequently, cells were then treated with and without 4-NP as described above. The medium was removed and the cells were washed with PBS and then with 0.5-1 mL of lysis buffer (10mM Tris-HCL, pH 7.9, 1.5 mM $MgCl_2$, 0.3 M sucrose, 1mM DTT and protease inhibitor cocktail). Cells were scraped with a cell scraper, sonicated for 1 min, followed by centrifugation at 12,500 RPM (Eppendorf Minispin Plus) for 8 min at room temperature. Supernatants represent whole-cell protein extracts. Protein concentrations were determined using the Bradford Assay and samples were prepared for immunoblotting.

2.4. Co-immunoprecipitation (Co-IP) methodology

Cellular fractions were incubated with anti-Gβ-protein specific antibody (rabbit polyclonal anti-Gβ, Santa Cruz Biotechnology, Santa Cruz, CA) for 1 h at 4 °C, followed by the addition of 100 µL 50% protein A-sepharose (Amersham Biochemical, Piscataway, NJ), pre-equilibrated in 10 mM Tris-HCl, pH 8.0 at 4 °C, and followed by the addition of protein A-sepharose for 2 hours. Samples were then centrifuged at 10,000 x g for 6 min and the pellets were washed with wash buffer (25mM Tris-HCL pH 7.2, 150mM NaCl), centrifuged for 8 min at 12,000 RPM (Eppendorf

Minispin Plus) at room temperature. The washing and centrifuging process was repeated 5 times and then 100µL of 1X SDS Laemmli sample buffer was added and then boiled in a water bath for 5 min. The samples were centrifuged and IP fractions were subjected to immunoblotting.

2.5. Electrophoresis and Immunobloting

Samples for immunoblotting were subjected to SDS-polyacrylamide gel (10%) electrophoresis followed by electro-transfer to a nitrocellulose membrane. The nitrocellulose membranes were incubated in 5% non-fat dry milk in Tris Buffered Saline (TBS) (10 mM TrisHCl and 150 mM NaCl, pH 7.4) for 1 hour at room temperature followed by overnight incubation with rabbit polyclonal anti-Gβ, and mouse monoclonal anti-α-tubulin (from Santa Cruz Biotechnology). The membranes were washed with 0.05% Tween 20 in TBS (TBST) and incubated with HRP-conjugated secondary antibodies (anti-rabbit IgG, anti-mouse IgG from Promega (Madison, WI), (1:1000)) in 0.01% BSA in TBST for 1 hr at room temperature. For sensitive detection, chemilluminescence (ECL) technique (SuperSignal West Pico Chemiluminescent Substrate) was used according to manufacturer's (Pierce Biotechnology, Rockford, IL) instructions. Quantitative analysis was done using LabWorks image acquisition and analysis software (UVP Laboratory Products, Upland, CA).

2.6. Confocal Microscopy and Immunostaining

PC12 cells were allowed to attach to immunocytochemistry slides (Lab-TEK II mounted on glass slides, VWR) or to coverslips placed in 12-wells plates and were grown overnight in DMEM with bovine calf serum and penicillin-streptomycin as described above. They were then treated with or without NGF, and 5 or 10µM 4-Nonylphenol for 1 hr or overnight. Cells were subsequently fixed

with previously cooled (-20ºC) 100% methanol. The cells were rinsed three times in 1% NGS (normal goat serum) (Sigma-Aldrich) in PBS and blocked for 1 hr at room temperature in 5% NGS in PBS. They were followed with incubation with primary antibodies in PBS with 1% NGS for 1-2 hours at 4 °C (mouse monoclonal anti-tubulin, and/or rabbit polyclonal anti-Gβγ). The slides were rinsed as before and incubated for 2 hrs with secondary antibodies (Alexa Fluor 488, Alexa Fluor 568, Alexa Fluor 405) (Molecular Probes-Invitrogen, Carlsbad, CA) in the dark to diminish photo-bleaching effects. The slides were rinsed and mounted with ProLong Gold antifade reagent with DAPI. High resolution, digital, fluorescent images were captured employing inverted, confocal laser scanning microscopy (model LSM 700; Zeiss, New York), utilizing a Plan-Apochromat 63x/1.40 immersion-oil DIC objective and assisted with ZEN 2009 software (Zeiss, New York, NY). Alexa Fluor 350 (blue), FITC (green), and rhodamine (red) were excited with laser emissions at 405-, 488-, and 555-nm wavelengths, respectively.

2.7. Statistical analysis

All statistical analysis was performed using Sigma Plot 11 software. In the case of Western-blot quantitative analysis, the differences between controls and treatments were assessed by means of the student's paired t-test. For comparisons between two groups, the student's paired t-test was employed. In all cases, a value of $p < 0.05$ was considered to be statistically significant.

2.8. Sample Preparation for Proteomic analysis

PC12 cells were grown on four 100-mm plates to 80% confluence over 2 days. The plates were then treated with (3, 4, 5, & 6) or without (plates 1 and 2) NGF for two consecutive days, followed by treatment with 10 μM 4-NP (plates 5 and 6) and NGF for an additional day. The Cytoskeletal

(CSK) and soluble (SOL) fractions were then prepared by extracting soluble proteins in an MT -stabilizing buffer (MS) (0.1 M PIPES, pH 6.9, 2 M glycerol, 5 mM MgCl2, 2 mM EGTA, 0.5% Triton X-100, protease inhibitor cocktail (Sigma-Aldrich), 0.1 mM GTP, and 1 mM DTT). Briefly, cells were rinsed and incubated with MS buffer (0.5–1 ml) for ~10 min at room temperature until cells began to lyse. Subsequently, cells were removed using a cell scraper and centrifuged at 10,000 × g for 10 min. The supernatant constitutes the SOL fraction, and the cell pellet represents the CSK fraction.

2.9. LC–MS/MS analysis

Protein pellets were re-suspended in 100 uL 0.4 M NH4HCO3 containing 8M urea and reduced with 5 mM DTT for 30 min at 55°C. Reduced thiol groups were alkylated with 10 mM iodoacetamide for 30 min at room temperature, and diluted 8-fold to a final concentration of 1M urea, 50mM NH4HCO3. The samples were digested overnight at 37°C with sequencing grade trypsin (Sigma-Aldrich). After quenching the reaction with TFA to a final concentration of 0.05% TFA, the samples were desalted with 100mg C18 cartridges (Supelco) and dried in a vacuum centrifuge.LC–MS/MS analyses were performed on an Ultimate 3000 RSLCnano system online coupled to a Q-exactive (Thermo Scientific). Peptides were introduced to the analytical column (Acclaim® PepMap RSLC, 75 μm × 15 cm, nanoViper, C18, 2 μm, 100 Å) and separated using a 90 min gradient from 5 to 40% solvent B at a flow rate of 300 nl/min (solvent A: 0.1% formic acid 5 % acetonitrile, solvent B: 0.1% FA 80% acetonitrile). The mass spectrometer was operated in a data-dependent mode. Full scan MS spectra were acquired at a mass resolution of 70,000 (mass range 400–1600 m/z and a target value of 1E6) in the Orbitrap analyzer. Tandem mass spectra of the 10 most abundant peaks of a full scan MS spectrum were acquired following peptide

fragmentation using higher-energy collisional dissociation (HCD) at a mass resolution 17,500 (target value of 2E5, NCE 28%, isolation width 4 m/z). The dynamic exclusion time was 15 s.

2.10. Protein identification

Protein quantification was performed using Proteome Discoverer 2.1 using the Rattus Norvegicus database downloaded in FASTA format from Uniprot on April, 2017. Protein statistical analysis was performed with Scaffold and Scaffold perspectives with 95% confidence and a minimum of 2 peptides. Log2 fold-change with ANOVA test were applied to obtain significant proteins ($p < .05$) and quantify down and up regulation.

CHAPTER 3: RESULTS

3.1 Specific Aim 1: Determine if 4-nonylphenol alters MTs and neuronal differentiation through Gβγ mediated pathway.

3.1.1 Objective and Overview

Dynamic rearrangements of MTs are critical for growth cone motility and neurite outgrowth. Recent results from our laboratory indicate that Gβγ, regulates neuronal outgrowth and differentiation by modulating microtubule (MT) assembly (Sierra-Fonseca, 2014). In Specific Aim 1, I explored the role of 4-NP on the expression of tubulin and Gβγ, MT assembly, and the interactions between Gβγ and tubulin/MTs during neuronal outgrowth and differentiation of PC12 cells.

3.1.2 4-NP alters tubulin expression but does not alter Gβγ expression in NGF-differentiated PC12 cells.

To determine if 4-NP affects tubulin or Gβγ expression in NGF-differentiated PC12 cells, PC12 cells were treated with NGF over the course of two to three days to allow for neuronal differentiation followed by treatment with 4-NP as indicated in the figure (**Fig. 5.1**). Whole cell lysates (WCL) were prepared as indicated in the methods. The samples were then processed for western blotting using anti-tubulin and anti-Gβ (**Fig. 5.1**). This experiment was repeated a total of three times and statistical analyses were carried out using one-way ANOVA. Controls represent 100%. Tubulin expression was significantly affected by 4-NP treatment (**Fig. 5.1A**) while Gβ expression remained unaltered (**Fig. 5.1B**). The reduction of tubulin after 4-NP treatment is

consistent with the idea that 4-NP inhibits neuronal differentiation by altering MTs/tubulin. The differences in the mean values among the treatment groups (A) are greater than would be expected by chance; there is a statistically significant difference ($P = 0.028$). The differences in the mean values among the treatment groups (B) are not great enough to exclude the possibility that the difference is due to random sampling variability ($P = 0.679$).

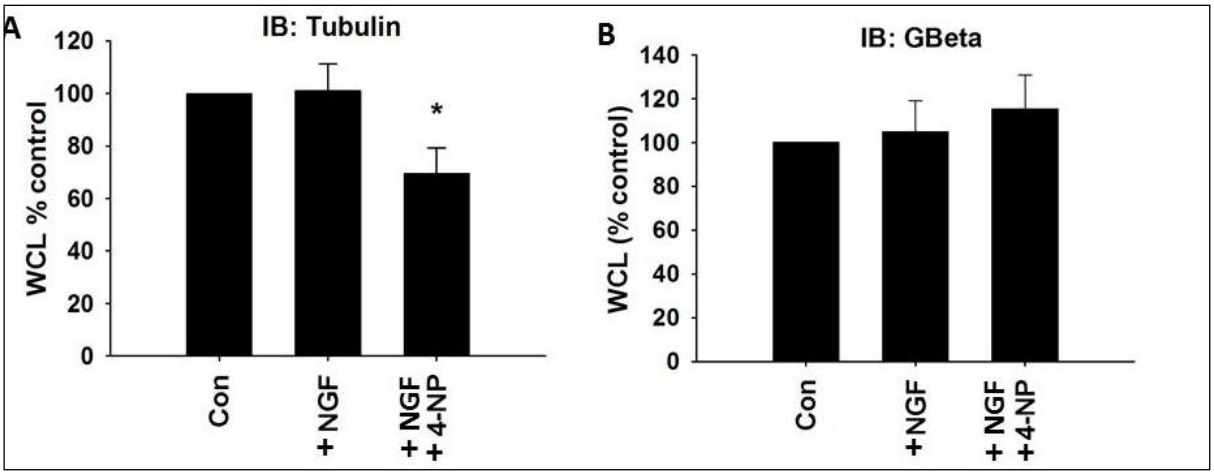

[Fig. 5.1 Effect of 4-NP in the expression of Tubulin and Gβγ .

Effect of 4-NP on the expression of Tubulin and Gβ in NGF differentiated PC12 cells. PC12 cells were treated with 100 ng/mL of NGF for two consecutive days to allow for differentiation. Subsequently, cells were treated with or without 4-NP overnight or for 1hr (acute treatment). Whole cell lysates were prepared as described in the methods. Equal amounts of proteins from each sample were subjected to immunoblot analysis using anti-Tubulin or anti-Gβ antibody as indicated. Protein bands were detected using the ECL-plus reagent, quantitated, and expressed as indicated in the figure.]

3.1.3 4-NP inhibits the interaction of Gβγ with tubulin in NGF-differentiated PC12 cells

To determine if 4-NP interferes with the interactions of Gβγ with tubulin during neuronal differentiation, PC12 cells were treated with NGF over the course of two to three days (to allow for neuronal differentiation) followed by treatment with 4-NP as indicated in the figure (**Fig. 6.1**). Whole cell lysates (WCL) were prepared as indicated in the methods. Samples were then subjected to co-IP using anti-Gβ or anti-tubulin antibodies followed by western blots using anti-Gβ or anti-tubulin antibody. The result indicates that NGF promoted the interactions of Gβγ with tubulin and the effect was blocked by 4-NP. When immunoprecipitation was carried out using anti-tubulin antibody followed by immunoblot analysis using anti-Gβ antibody, 4-NP was found to have a similar effect on tubulin-Gβγ interaction. After NGF treatment, Gβ interaction with tubulin increased similarly to the NGF treated cells in **Fig. 6.1**. The results shown also support that 4-NP inhibits the Gβγ interaction with tubulin.

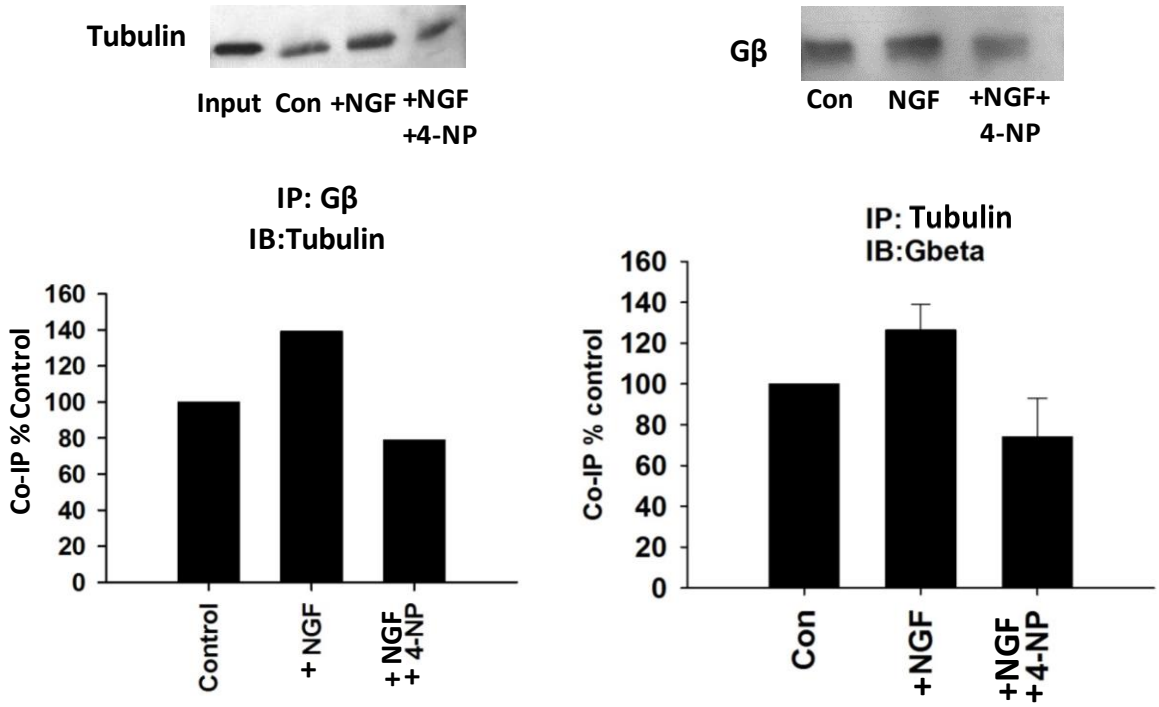

[Fig. 6.1. Interaction between tubulin and Gβ is affected by 4-NP treatment.

The PC12 cells were treated with NGF as indicated in the methods. Subsequently the cells were treated with 5µM 4-NP. The whole cells lysates were prepared and subjected to immunoprecipitation using anti-Gβ, and anti-tubulin antibodies followed by western blots using anti-tubulin and anti-Gβ antibody as described in the methods. Protein bands were quantitated and expressed percent Gβ co-immunoprecipitated with tubulin and tubulin co-immunoprecipitated with Gβ with control representing 100%.]

3.1.4 4-NP alters Polymer-monomer (MT/tubulin) equilibrium.

We evaluated the effect of 4-NP in PC12 cells to understand the role of 4-NP and its link to MT assembly. To conduct the experiment, PC12 cells were treated with or without NGF as indicated in the methods. Subsequently, cells were treated with or without 10μM 4-NP. Cytoskeletal (CSK, enriched in MTs) and soluble protein fractions (SOL, enriched in dimeric tubulin) were separated as indicated in the methods. MT assembly was assessed by calculating the % of Tubulin in CSK fraction. We found that MT-assembly was increased in PC12 cells after treatment at 10μM 4-NP (Figure 7.1). Previous studies indicated that Gβγ associates with microtubules and this association is important for microtubule assembly (Roychowdhury and Rasenick., 1997; Montoya et. al., 2007). Therefore we determined if Gβγ association with MTs was altered after 4-NP treatment. We found that Gβ was associated with MTs and 4-NP did increase the association.

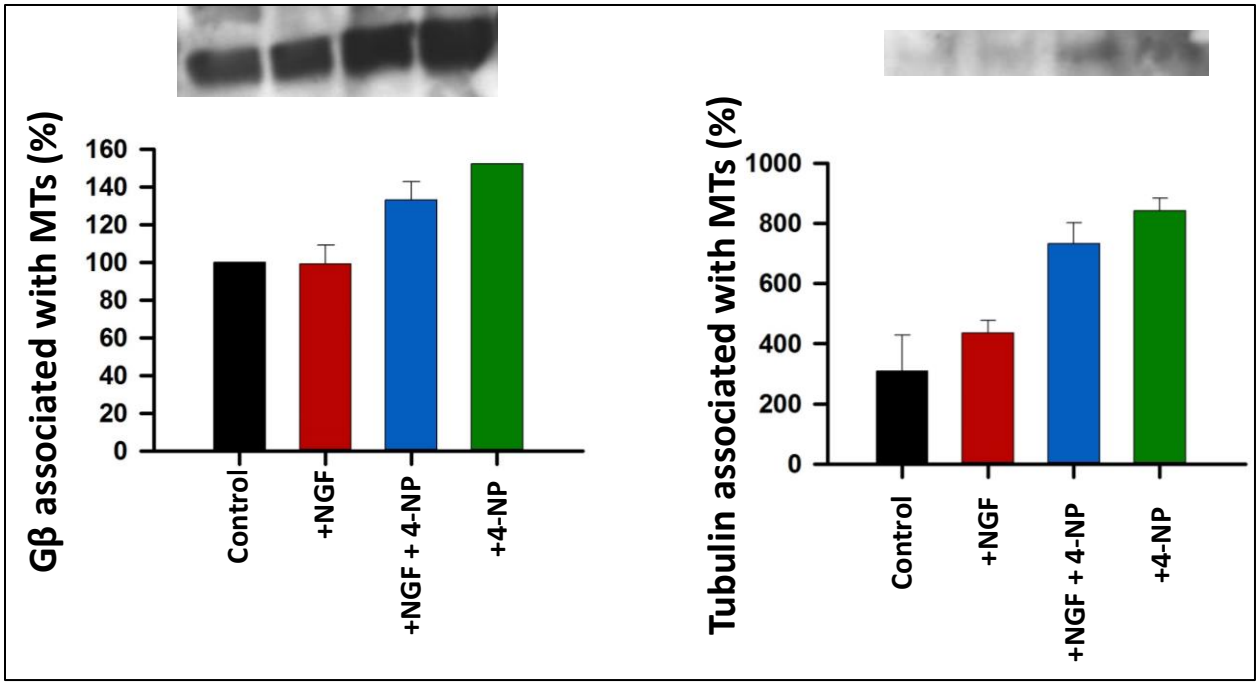

[Fig. 7.1. Gβ and Tubulin association with Microtubules.

PC12 cells were treated with 4-NP at a concentration of 10μM for 24 hours. After incubation, subcellular fractionation was performed and CSK fractions were subjected to Western blot using anti-Gβ and anti-tubulin antibody as indicated in the methods. Protein bands were detected using the ECL-plus reagent and quantitated. MT assembly was determined by assessing tubulin immunoreactivity in the CSK fraction, and it is expressed as percent tubulin in CSK fraction. The graphic shows percent Gβ and tubulin in CSK fractions. Values shown represent mean ± standard error of two independent experiments done in duplicates. No significant change was found.]

3.1.5. Confocal microscopic analysis indicates 4-NP disrupts MT and Gβγ organization, cellular morphology and neurite formation

To determine the effect of 4-NP in MT and actin organization as well as neurite formation, PC12 cells were treated with 100 ng/mL of NGF for two consecutive days to induce neurite outgrowth. Subsequently, 5 µM 4-NP was added to the media and the cells were incubated overnight as indicated in the figure legend (Fig. 8.1). The cells were then fixed and triple labeled with monoclonal anti-tubulin (red), anti-actin (green) and polyclonal anti-Gβ (blue) antibodies, and processed for confocal microscopy (Fig. 8.1). In control cells (in the absence of NGF), Gβγ co-localized with MTs and actin filaments in the cell body. After NGF treatment, the majority of the cells displayed neurite formation. Gβγ was detected in the neurites and in cell bodies, where they co-localized with MTs and actin filaments. In the presence of 4-NP, neurite formations were inhibited. Normal organization and localization of MTs, actin filaments, and Gβγ were altered. The microtubules were pushed towards the membrane and the cells were rounded. MT intensity in the cells was also reduced. Actin cytoskeleton was found to be damaged and actin immunoreactivity was detected all over the cells including nucleus. The results clearly suggest that 4-NP has a very damaging effect on the cytoskeletal arrangement in NGF-differentiated PC12 cells. The results further suggest that interaction of Gβγ with tubulin/actin is important for integrity of MTs/actin filaments, and 4-NP causes cytoskeletal disruption by inhibiting/altering these interactions. At a higher concentration, 10 µM, 4-NP had more damaging effects on neurite formation (Fig. 9.1). The cells that were treated after incubation with NGF had curly processes and altered expression/localization of Gβ. Meanwhile, the cells that were treated with both NGF and 10 µM 4-NP (Co-incubation), retained the straight process shape (Fig. 9.1, lower panel).

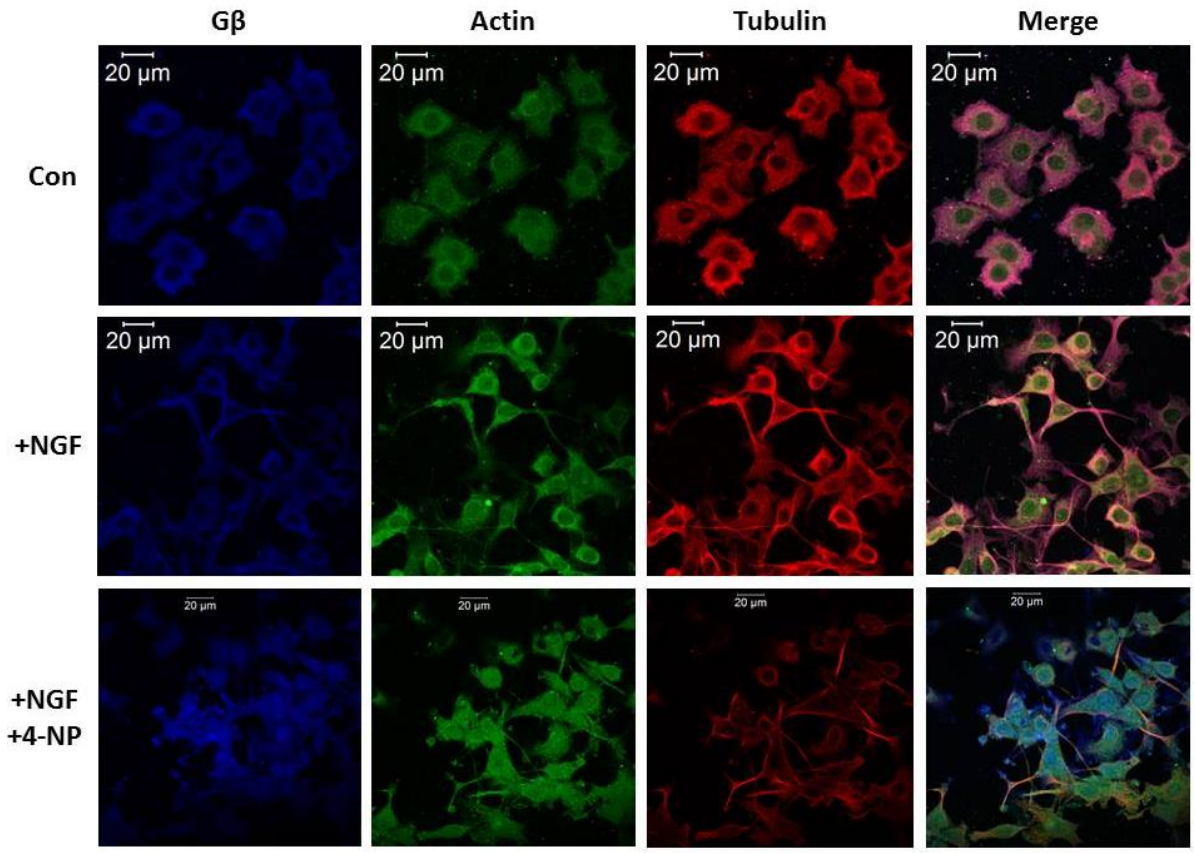

[Fig. 8.1. Effect of 4-NP on cytoskeletal organization, and association of Gβ, microtubules and actin filaments in NGF-differentiated PC12 cells.

PC12 cells were allowed to differentiate in the presence of NGF followed by treatment with 4-NP for one day. Samples were processed for confocal microscopy using anti-Gβ (blue), anti-actin (green), and anti-tubulin (red). In NGF treated cells, neurite outgrowth was observed. Co-localization between Gβ and tubulin was observed mainly in the neuronal processes in the 4-NP treated cells. Actin was localized all over the neurite in the 4-NP treated cells as compared to the NGF treated cells where it was mainly localized in the cytoskeleton.]

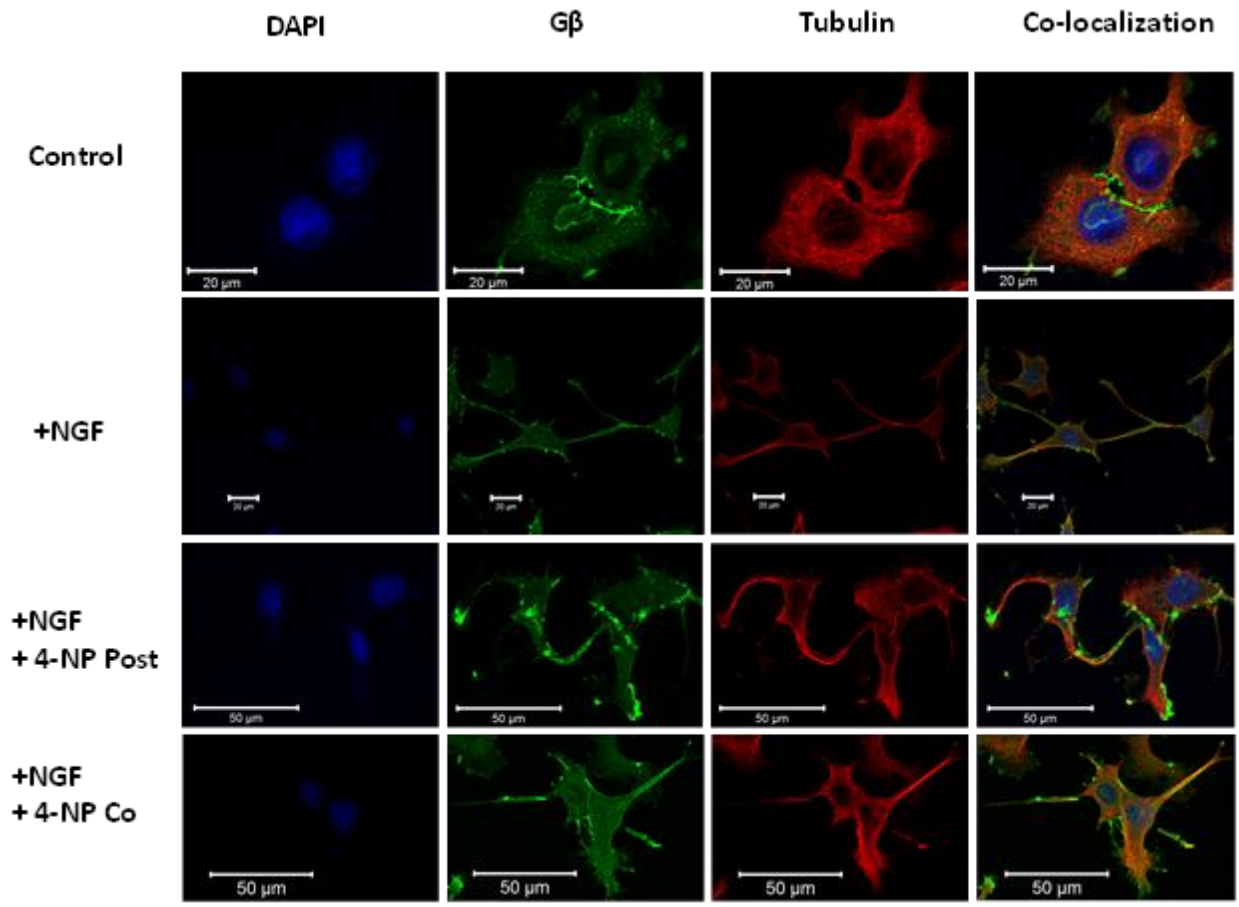

[Fig. 9.1. Effect of 4-NP post-incubation and co-incubation with NGF.

PC12 cells were allowed to differentiate in the presence of NGF followed by treatment with 4-NP for one day. Samples were processed for confocal microscopy using anti-Gβ (green), and anti-tubulin (red). Blue represents nuclear labeling.]

3.2 Specific Aim-2: Examine the cytoskeletal alterations and neurodegeneration induced by 4-nonylphenol.

3.2.1 Objective and Overview:

Cytoskeletal defect followed by its dysfunction, are hallmark of neurodegeneration (McMurray CT 2000). Previous studies from our laboratory and the preliminary results from Specific Aim-1 indicate that 4-NP inhibits neurite outgrowth from PC12 cells, alters MT and Gβγ organization, and induces cellular aggregation and degeneration. In addition, interactions between Gβγ and tubulin/actin were inhibited in the presence of 4-NP. These results suggest that 4-NP might induce neurodegeneration by altering dynamic behavior of cytoskeleton. Neuronal cytoskeleton consisting of MTs, actin filaments, and neurofilaments and a large number of CSK-associated proteins, is highly dynamic in nature with an inherent ability to assemble and disassemble in response to diverse signals. The identity of many of these proteins and signaling molecules and how they network spatially within the cell to regulate cytoskeleton remodeling is not well understood. Therefore, to better understand the role of 4-NP in the disruption of the cytoskeleton and neurodegeneration, in specific aim-2, I will conduct proteomic analysis of cytoskeletal fraction. I will also determine whether 4-NP alters expression/localization/phosphorylation of tau proteins in NGF differentiated PC12 cells. Tau is a microtubule-associated protein found only in axons and it is known to regulate MT assembly and neurite outgrowth. Abnormal phosphorylation of tau and its aggregation is associated with several human neurodegenerative disorders known as taupathies (Alonso, 2008; Amniai, 2008; Gustav-Rothenberg, 2010).

3.2.2 Proteomic analysis of cytoskeletal fraction reveals that 4-NP downregulated tubulin/actin but upregulated significantly G protein subunits including β1 and β2 in NGF-differentiated PC12 cells.

Proteomic Analysis by mass spectrometry provides a valuable tool to analyze the large numbers of proteins in complex samples. Cytoskeleton (CSK) is composed of three major protein filaments: actin filaments, microtubules and intermediate filaments. In addition, several microtubules and actin-associated proteins, a large number of proteins including motor proteins are also integral component of neuronal cytoskeleton. Therefore, we have conducted proteomic analysis of CSK from control and 4-NP treated PC12 cells (both in the presence and the absence of NGF). CSK fractions were subjected to LC-MS/MS analyses in the Orbitrap analyzer as described in the methods. Protein identifications were performed with Scaffold-Perspective software. As expected, many cytoskeletal proteins were identified in cytoskeletal fractions of control PC12 and NGF-differentiated PC12 cells and many of them were up/down regulated in the presence of 4-NP. The Heatmap analysis (Fig. 10.1) which shows up- and down-regulation of cytoskeletal proteins compared to control PC12 cells. We found that ~ 500 proteins associated with CSK were up/down-regulated in the presence of NGF (control vs NGF), and ~335 proteins were up/down-regulated in the presence of 4-NP (NGF vs NGF+ 4-NP). Few of these proteins (relevant to our study) are shown in **Table 1.1**. As shown in the table, several tubulin/actin isotypes were found in the cytoskeleton fraction with a high score (high spectral count) reflecting the abundance of these isotypes in CSK. As expected, all tubulin and actin isotypes, microtubule-associated protein isotypes, were significantly upregulated (shown by single asterisk) in the presence NGF. All of them were down-regulated in the presence of 4-NP as shown by spectral

count but only few are statistically significant as shown by double asterisk. Interestingly beta 3 tubulin (Table 1.1), a neuron-specific tubulin isotype was upregulated in the presence of NGF supporting further that NGF is inducing neuronal phenotype in PC12 cells. As shown in the Table Several Microtubule-associated proteins were significantly up-regulated in the presence of NGF. These proteins are known to promote and stabilize MTs and are very important for neuronal functions. 4-NP did not significantly affect the expression level of most of these proteins. Among the tubulin isotypes, Tubulin beta 3 isotype (neuron-specific protein) was slightly up-regulated in the presence of 4-NP, while beta chain was slightly down-regulated. Among microtubule-associated proteins (MAPs), most MAPs (MAP2, MAP1A and 1B) were not affected by 4-NP. Interestingly, MAP 4, which was not significantly affected by NGF was up-regulated in the presence of 4-NP (Table 1.1).

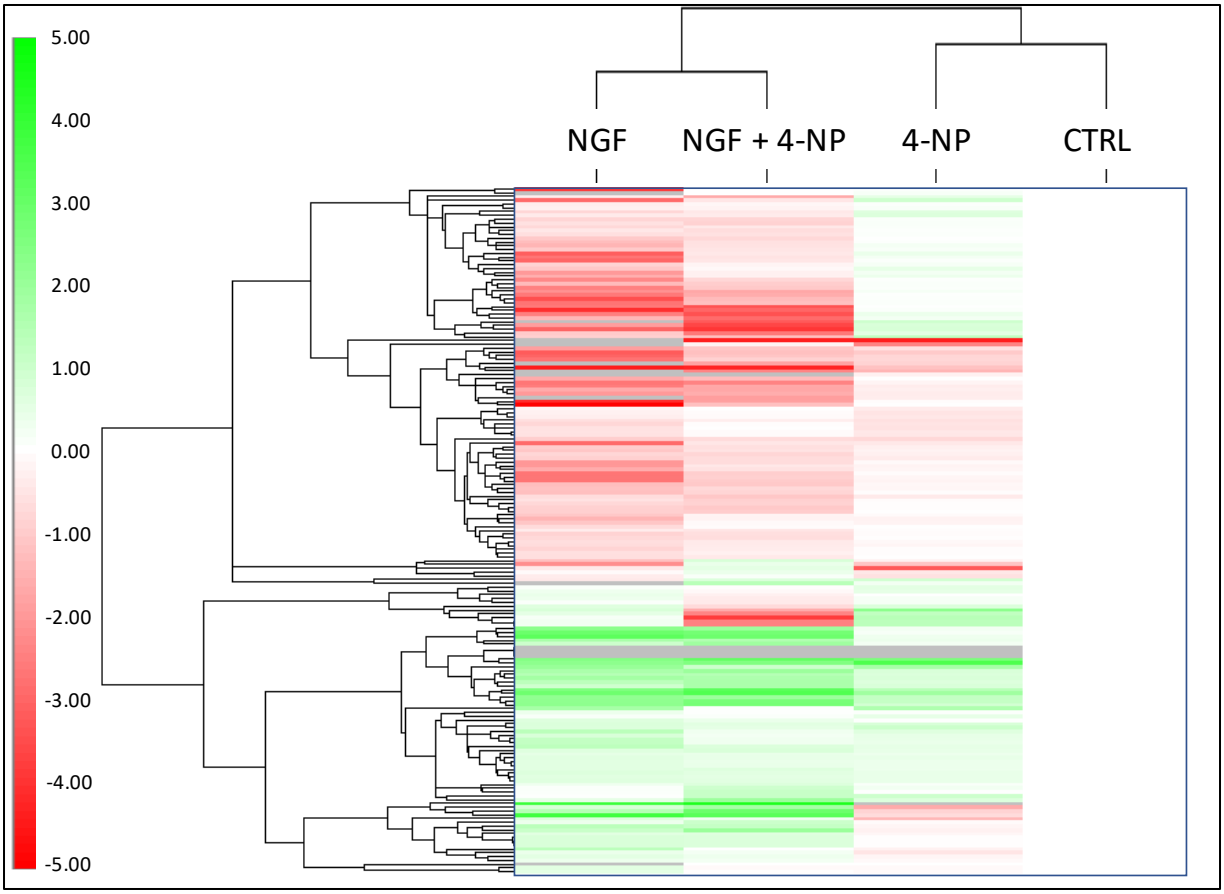

[Fig. 10.1 Heat map analysis of CSK proteins.

The Heatmap analysis shows up- and down-regulation of cytoskeletal proteins compared to control PC12 cells. We found that ~ 500 proteins associated with CSK were up/down-regulated in the presence of NGF (control vs NGF), and ~335 proteins were up/down-regulated in the presence of 4-NP (NGF vs NGF+ 4-NP).]

Regarding G protein subunits, Gβ1 and Gβ2 were consistently associated with CSK fractions in PC12 cells (control and NGF-differentiated) and significantly up-regulated in the presence 4-NP (Table 1.1). This is an interesting observation because 4-NP was shown to inhibit neurite outgrowth, induce cellular aggregation and degeneration in Gβγ overexpressed PC12 cells (Martinez, UTEP-MS thesis 2013). Therefore, it is likely that upregulation of Gβ observed in the presence of 4-NP might have played an important role in cytoskeletal disruption and neuronal damage observed in 4-NP-exposed cells. Interestingly, both heavy and light chain of kinesin (a motor protein) and actin-related protein 2/3 were differentially regulated by NGF/4-NP. We also determined the effect of 4-NP in CSK of control PC12 cells, and found that several isotypes of tubulin (beta 5, beta chain, alpha 1C) were (Log2 fold change ~0.28) upregulated in the presence of 4-NP. Among the MAPs, MAP4 was significantly upregulated (Log2 fold 1.37) in the presence of 4-NP. Interestingly, no changes in G protein subunits, β1 and β2 subunits were observed in the CSK fraction in the presence of 4-NP.

We also carried out proteomic analysis of whole cell lysates (WCL) preparations from control, NGF differentiated and 4-NP treated cell (Table 2.1). Table shows the cytoskeletal proteins, and G protein subunits that are significantly up- or down-regulated in WCL. We found that most of the tubulin isotypes that were up-regulated in CSK in response to NGF were also increased in WCL. However, unlike CSK where several MAPs were up-regulated, only MAP1B was upregulated in WCL. Most surprisingly, all G protein subunits were significantly down-regulated in the presence NGF in WCL. We found that unlike CSK fractions, 4-NP did not have any significant effects on the expression of these proteins in WCL. Only protein that was affected by 4-NP was MAP4. However, 4-NP significantly down-regulated many proteins including several

G protein subunits. Therefore, it appears that despite down-regulation of G protein subunits in WCL, these subunits were up-regulated in CSK.

TABLE 1.1 Effect of NGF and 4-NP on the upregulation/downregulation of proteins in Cytoskeletal Fractions (Spectral Count) of PC12 cells

PROTEIN ID	M.Wt (kDa)	Accession Number	CON	+NGF	+NGF + 4-NP	Log2 Fold	Fold Change
Actin, cytoplasmic	42	ACTB_	4265	6246*	4793	0.187*	1.14
Actin	50	AOAOG2K3K2	4248	6220*	4767	0.186*	1.14
Actin, alpha skeletal	42	ACTS	1129	2057*	1316**	0.551* -0.661**	1.47 0.63
Tubulin beta-5 chain	50	TBB5	2097	3849*	3456	0.478*	1.4
Tubulin beta chain	50		853	1557*	1445	0.564*	1.50
Tubulin beta-4B chain	50	TBB4B	1575	2995*	2740	0.615*	1.53
Tubulin alpha-1C chain	50	TBA1C	1408	2683*	2232	0.551*	1.47
Filamin A	280		1120	1868	1306		
Guanine nucleotide-binding protein subunit beta-2	37	GBB2	58	72	103**	0.62 **	1.53
Guanine nucleotide-binding protein subunit beta-1	37	GBB1	45	56	89**	0.812**	1.76
Guanine nucleotide-binding protein G(i) subunit alpha-2	41	GNA12	11	27	37		
Guanine nucleotide-binding protein G(o) subunit alpha	40	GNA0	3	6	10		
Guanine nucleotide-binding protein G(k) subunit alpha	41	GNAI3	1	3	13**	2.18**	4.53
Kinesin-1 heavy chain	110	KINH	18	5	22**	2.24**	4.72
Microtubule-associated protein 1A	300	MAP1A	1	17*	10	3.76*	13.5
Microtubule-associated protein 1B	270	F1LRL9	4	22*	20	2.13*	4.38
Microtubule-associated protein 4	110	MAP4	11	34	53**	0.799**	1.71
Actin-related protein 2/3 complex subunit 1A	42	ARC1A	111	64*	78	-1.18*	0.44

* Control vs NGF ** NGF vs NGF+4-NP

TABLE 2.1 Effect of NGF and 4-NP on the upregulation/downregulation of proteins in WCL Fractions (Log 2) of PC12 cells

PROTEIN ID	Accession Number	WCL		
		Control vs NGF	NGF vs NGF + 4-NP	Control vs 4-NP
Actin, cytoplasmic 1	ACTB_	0.331		-0.44
Actin	AOAOG2K3K2	0.331		-0.44
Actin, alpha skeletal	ACTS			
Tubulin beta-5 chain	TBB5	0.563		
Tubulin beta chain	G3V7C6	0.51		
Tubulin beta-4B chain	TBB4B			
Tubulin alpha-1C chain	TBA1C	0.865		
Filamin A	C0JPT7			-0.654
Guanine nucleotide-binding protein subunit beta-2	GBB2			-0.697
Guanine nucleotide-binding protein subunit beta-1	GBB1	-0.459		-0.721
Guanine nucleotide-binding protein G(i) subunit alpha-2	GNA12	-1.31		-1.91
Guanine nucleotide-binding protein G(o) subunit alpha	GNA0	-1.41		-1.72
Guanine nucleotide-binding protein G(k) subunit alpha	GNAI3			-2.12
Kinesin-1 heavy chain	KINH			
Microtubule-associated protein 1A	MAP1A			
Microtubule-associated protein 1B	F1LRL9	1.06		-1.68
Microtubule-associated protein 4	MAP4		0.711	-0.979
Actin-related protein 2/3 complex subunit 1A	ARC1A	-2.18		

3.2.3. Top ten proteins most affected by 4-NP (up- and down-regulated) in CSK in control and NGF-differentiated PC12 cells

To understand the mechanisms by which 4-NP alters CSK, we identified most affected proteins (up or down-regulated) from proteomic analysis. Top ten up and down regulated proteins in the CSK fraction are shown in Table 3.1. These affected proteins include Cbr1 (NADPH), MAP1a, Huntington Interacting protein 1, and Mitochondrial ribosomal protein L13. The gene Cbr1 encodes for carbonyl reductase 1 which according to several studies suggest that CBR1 represents a significant pathway for the detoxification of reactive aldehydes derived from lipid peroxidation and that CBR1 in humans is essential for neuronal cell survival and to confer protection against oxidative stress-induced brain degeneration (Rashid, 2016). Interestingly, this gene is downregulated in NGF treated cells but is upregulated in NGF treated cells that were subsequently treated with 4-NP. The MAP1a gene encodes for a protein that is believed to be involved in microtubule assembly. Previous studies have indicated that disruption of MAP1a could be a very early manifestation of Aβ-mediated synaptic dysfunction—one that presages the clinical onset of AD by years (Clemmensen, 2012). This gene is shown to be upregulated in NGF treated cells by 3.76 log2 fold. Although neurodegenerative diseases exhibit distinct pathological features, abnormal endocytic trafficking is apparent in several neurodegenerative diseases, such as Alzheimer's disease, and Parkinson's disease (Wang et al., 2014). Huntington interacting protein 1 has been shown to be involved in clathrin-mediated endocytic trafficking and is downregulated in the presence of 4-NP.

TABLE 3.1 Top 10 Up and down regulation of proteins after NGF or NGF + 4-NP treatments in CSK

CSK	Protein ID	Accession Number	Log2 fold #
Downregulated Control vs NGF	Carbonyl reductase [NADPH] 1	CBR1_RAT	-5.24
	Transcription initiation factor TFIID subunit 9	A0A096MJG1_RAT	-4.72
	Group of Transcription initiation factor TFIID subunit 9B	A0A0G2JXE2_RAT (+2)	-4.42
	Fatty acid synthase	FAS_RAT	-4.17
	Exportin-1	XPO1_RAT	-4.08
	Zinc finger, C3HC-type-containing 1	A0A140UHX2_RAT	-4.03
	Transcription initiation factor TFIID subunit 6	TAF6_RAT	-4.03
	Group of Bleomycin hydrolase	A1A5L1_RAT (+1)	-3.91
	Nitrilase 1, isoform CRA_a	F7ESM5_RAT	-3.79
	Trifunctional purine biosynthetic protein adenosine-3	G3V918_RAT	-3.65
Upregulated Control vs NGF	RCG45489, isoform CRA_a	Q5XI04_RAT	3.18
	Glypican 6	A0A096MJY1_RAT	3.26
	WD repeat domain 26	F1LTR1_RAT	3.37
	60S ribosomal protein L14	F1LSW7_RAT	3.48
	Serotransferrin	A0A0G2QC06_RAT	3.58
	Dystonin	D3ZC56_RAT	3.72
	Microtubule-associated protein 1A	MAP1A_RAT	3.76
	Inositol 1,4,5-trisphosphate receptor type 3	C7E1V1_RAT	3.84
	60S ribosomal protein L5	RL5_RAT	3.99
	60S ribosomal protein L3	RL3_RAT	3.99
Downregulated NGF vs NGF + 4-NP	AP-2 complex subunit alpha-2	Q66HM2_RAT	-4.09
	Golgin A3	D3ZLD5_RAT	-3.7
	Cleavage stimulation factor subunit 3	F1M4W7_RAT	-3.17
	Huntingtin interacting protein 1, isoform CRA_a	G3V8Y8_RAT	-3
	Enhancer of mRNA-decapping protein 4	F7F707_RAT	-2.84
	Enhancer of mRNA-decapping protein 4	EDC4_RAT	-2.84
	DEAD-box helicase 6	D3ZD73_RAT	-2.81
	Cyclin-dependent kinase 2-associated protein	B0BN48_RAT	-2.66
	Adaptor protein complex AP-2, alpha 1 subunit (Predicted)	D3ZUY8_RAT	-2.5
	Group of Epsin 2	Q505I9_RAT (+2)	-2.46
Upregulated NGF vs NGF + 4-NP	Trifunctional purine biosynthetic protein adenosine-3	G3V918_RAT	3.32
	Mitochondrial ribosomal protein L13	Q5XFW4_RAT	3.32
	Group of 2-oxoisovalerate dehydrogenase subunit alpha	ODBA_RAT (+1)	3.32
	Mitochondrial ribosomal protein S18B	F6Q5K7_RAT	3.32
	Group of Mitochondrial ribosomal protein L1	F1M9A4_RAT (+2)	3.58
	Peptidylprolyl isomerase domain and WD repeat containing 1	D3ZVP6_RAT	3.58
	ATP-dependent Clp protease proteolytic subunit	M0RAD5_RAT	3.7
	Group of Bleomycin hydrolase	A1A5L1_RAT (+1)	3.81
	Carbonyl reductase [NADPH] 1	CBR1_RAT	3.91
	Threonine--tRNA ligase, cytoplasmic	A0A0G2K9V6_RAT	3.91

TABLE 4.1 Top 10 Up and down regulation of proteins after NGF or NGF + 4-NP treatments in WCL

WCL	Protein ID	Accession Number	Log2 fold #
Downregulated Control vs NGF	Epithelial protein lost in neoplasm	F1LR10_RAT	-4.69
	NADH-ubiquinone oxidoreductase 75 kDa subunit	NDUS1_RAT	-4.65
	Lamin B2	D3ZLC1_RAT	-3.64
	Protein FAM3C	FAM3C_RAT	-3.54
	Structural maintenance of chromosomes protein	D4A1B9_RAT	-3.37
	Group of Transcription activator BRG1	SMCA4_RAT (+1)	-3.37
	Group of Prostaglandin F2 receptor negative regulator	FPRP_RAT (+1)	-3.32
	Delta(3,5)-Delta(2,4)-dienoyl-CoA isomerase	ECH1_RAT	-3.28
	Mitochondrial pyruvate carrier 2	MPC2_RAT	-3.28
	Nucleoporin 205	D4A7R3_RAT	-3.28
Upregulated Control vs NGF	Ubiquitin-conjugating enzyme E2 Z	UBE2Z_RAT	3.22
	UMP-CMP kinase	KCY_RAT	3.44
	Kinesin family member 11	F1MAB8_RAT	3.44
	Niban-like protein 1	NIBL1_RAT	3.63
	Basic leucine zipper and W2 domain-containing protein 2	BZW2_RAT	3.63
	Group of Paxillin	A0A0G2JY12_RAT (+1)	3.63
	Group of S-adenosylmethionine synthase	Q6P688_RAT (+2)	3.95
	Zyxin	D4A7U1_RAT	4.33
	Glutathione synthetase	GSHB_RAT	4.33
	Armadillo repeat-containing 6	B2RYL4_RAT	5.09
Downregulated NGF vs NGF+ 4-NP	Golgi reassembly stacking protein 2	Q68G33_RAT	-3.72
	FLII, actin-remodeling protein	Q5RKI5_RAT	-3.27
	Keratin, type I cytoskeletal 10	A0A0G2K2V6_RAT	-3.13
	G1/S-specific cyclin-D1	CCND1_RAT	-2.81
	Group of GrpE protein homolog 1, mitochondrial	GRPE1_RAT (+1)	-2.62
	Squalene synthase	FDFT_RAT	-2.62
	Caspase 7	O88550_RAT	-2.62
	Casein kinase II subunit beta	CSK2B_RAT	-2.39
	Cytoplasmic dynein 1 light intermediate chain 1	G3V7G0_RAT	-2.39
	Coagulation factor V	A0A0G2K3W2_RAT	-2.27
Upregulated NGF vs NGF+ 4-NP	D-dopachrome decarboxylase	DOPD_RAT	1.57
	NADH dehydrogenase [ubiquinone] flavoprotein 2	NDUV2_RAT	1.68
	tRNA (guanine(26)-N(2))-dimethyltransferase	A0A140UHW6_RAT	1.78
	Histone H2A	D4AEC0_RAT	2
	Ribulose-phosphate 3-epimerase	A0A0G2JW38_RAT	2.19
	Nuclear autoantigenic sperm protein	NASP_RAT	2.44
	Nucleolar protein 3	G3V7Z3_RAT	2.78
	Cytochrome b-c1 complex subunit 7	B2RYS2_RAT	2.89
	Charged multivesicular body protein 5	CHMP5_RAT	3
	High mobility group nucleosome-binding domain 1	Q5U1W8_RAT	3.19

3.2.4. Principal Component Analysis

We also carried out **Principal component analysis** (**PCA**) using scaffold-perspective software to successfully separate out 4 clusters corresponding to different treatment conditions as shown in Fig. 11.1. It is clear from the figure that NGF-induced neuronal differentiation of PC12 cells has profound effect on altering protein profile of cytoskeleton of PC12 cells. However, it is also clear that 4-NP has significantly affected the protein composition/pattern of CSK in NGF-differentiated PC12 cells.

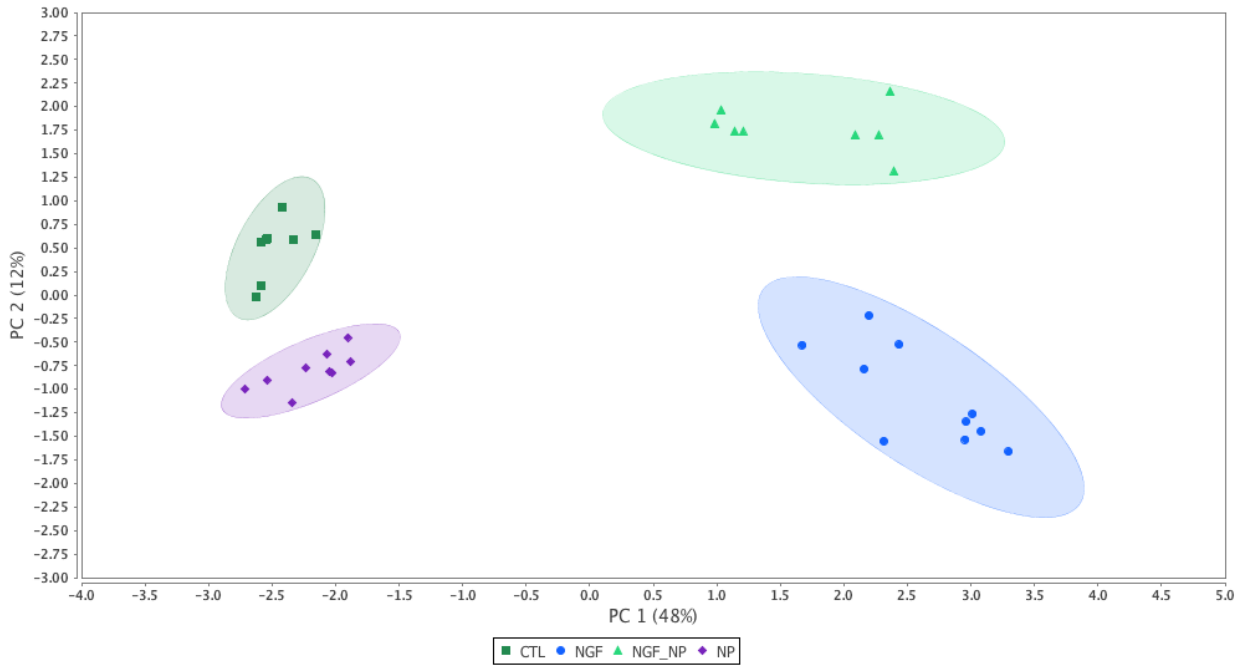

Fig. 11.1. PCA analysis showing 4 clusters showing the effect of 4-NP

3.2.5. String Link and gene ontology (GO) enrichment analysis

Scaffold Perspective software was also used to carry out gene ontology (GO) enrichment analysis. This analysis helps in identifying protein that are upregulated or downregulated under certain condition (or treatment), are associated with specific biological functions, i.e. to assess biological meaning with gene ontology. Fig. 12.1 shows that the several biological pathways are affected by upregulation of proteins by 4-NP in NGF differentiated PC12 cells. Some of the pathways that are relevant to cytoskeleton are shown in Table 5.1. Interestingly, KEGG pathway (Kyoto Encyclopedia of Genes and Genomes) shows Alzheimer's, Parkinson's, and Huntington disease pathways are affected by 4-NP treatment. KEGG is a collection of manually drawn pathway generated from large-scale molecular datasets generated by omic analysis. Two pathways, Alzheimer's Disease and Dopaminergic synapse pathways, from the KEGG pathway previously mentioned in Table 5.1, were affected by 4-NP treatment and are shown in Fig. 13.1. Several genes from these pathways are listed in Table 6.1. Several proteins of the succinate dehydrogenase subtypes, NADH subtypes, and ATP synthase subtypes, are affected by 4-Nonylphenol treatment and are found in various neurodegenerative diseases such as Alzheimer's, Parkinson's, and Huntington's. However, some proteins, such as Guanine nucleotide-binding protein G(k) subunit alpha and Calpain-2 catalytic subunit, are pathway specific (Table 6.1). The CSK proteins that were affected in control PC12 cells after 4-NP treatment are NADH dehydrogenase subtypes, succinate dehydrogenase subtypes, along with cytochrome c oxidase subtypes (Table 7.1). These proteins are known to be crucial to the survival and function of neural cells. The malfunction of mitochondria including cytochrome c oxidase, the terminal enzyme complex of the respiratory chain, increases ATP levels in neural cells and subsequently increases the production of reactive oxygen species (Arnold, 2012).

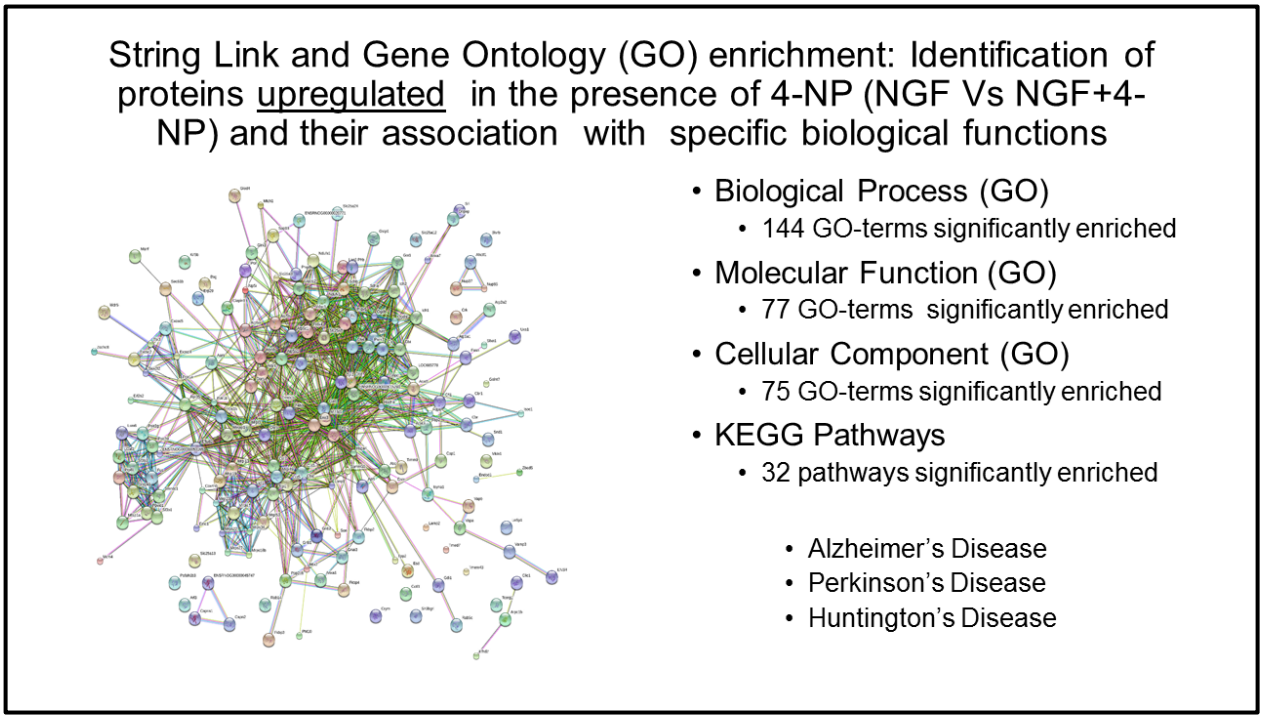

Fig. 12.1 String Analysis

Table 5.1 Biological pathways (shown by Gene Ontology) affected by upregulation of protein by 4-NP in NGF-differentiated PC12 cells.

Pathway ID	Pathway description	Count in gene set
GO: 0008092	cytoskeletal protein binding	9
GO: 0044444	cytoplasmic part	70
GO: 0005737	cytoplasm	82
GO: 0005856	cytoskeleton	17
GO: 0044430	cytoskeletal part	12
GO: 0015630	Microtubule cytoskeleton	10
GO: 0005874	microtubule	6
0512-KEGG pathway	Parkinson's disease	14
0516-KEGG pathway	Huntington's disease	14
0510-KEGG pathway	Alzheimer's disease	13
04728: KEGG pathway	Dopaminergic synapse	5

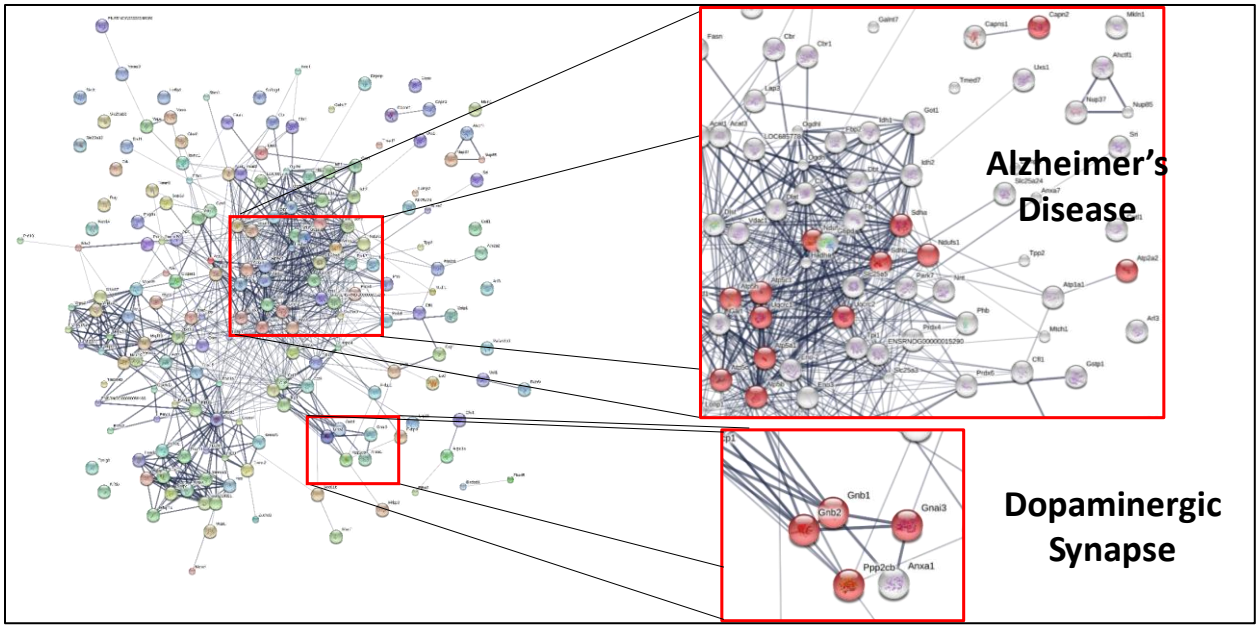

[Fig. 13.1. String Analysis showing Alzheimer's Disease and Dopaminergic Synapse pathways affected by 4-NP in CSK.

String link shows that several genes encoding for proteins involved in Alzheimer's disease, and Dopaminergic synapse are affected by 4-NP treatment.]

TABLE 6.1: Effect of NGF and 4-NP on the upregulation/downregulation of proteins in AD, PD and HD pathways in Cytoskeletal Fractions of PC12 cells

PROTEIN ID	**M.Wt (kDa)**	**Accession Number**	**CON**	**+NGF**	**+NGF + 4-NP**	**Log2 Fold**	**Pathways**
Succinate dehydrogenase [ubiquinone] flavoprotein subunit	72	SDHA_RAT	-	46	90	0.97**	AD, PD, HD
Succinate dehydrogenase [ubiquinone] iron-sulfur subunit	32	SDHB_RAT	-	21	36	0.78**	AD, PD, HD
NADH-ubiquinone oxidoreductase 7	79	NDUS1_RAT	-	212	226	0.092**	AD, PD, HD
NADH dehydrogenase (Ubiquinone) flavoprotein 1	51	Q5XIH3_RAT	104	63	115	-1.05* 0.87**	AD, PD, HD
Cytochrome b-c1 complex subunit 1	53	QCR1_RAT	-	168	201	0.26**	AD, PD, HD
Cytochrome b-c1 complex subunit 2	48	QCR2_RAT	-	111	132	0.25**	AD, PD, HD
ATP synthase subunit gamma	33	Q6PCU0_RAT	64	54	94	-0.57* 0.78**	AD, PD, HD
ATP synthase subunit alpha	60	ATPA_RAT	-	591	643	-0.24* 0.12**	AD, PD, HD
ATP synthase subunit beta	56	G3V6D3_RAT	767	810	910	-0.24* 0.17**	AD, PD, HD
ATP synthase subunit O	23	ATPO_RAT	47	35	75	-0.75* 1.1**	AD, PD, HD
Sarcoplasmic/endoplasmic reticulum calcium ATPase 2	115	AT2A2_RAT	-	10	26	0.23**	AD
Calpain-2 catalytic subunit	80	CAN2_RAT	-	25	36	-1.21* 0.53**	AD
ADP/ATP translocase 2	33	ADT2_RAT	-	131	157	0.23**	PD, HD
Protein DJ-1	20	PARK7_RAT	41	22	38	-1.23* 0.79**	PD
Guanine nucleotide-binding protein G(k) subunit alpha	41	GNAI3_RAT	-	3	13	2.07**	PD
DNA-directed RNA polymerase II subunit RPB7	19	RPB7_RAT	33	23	34	0.56**	HD
Polymerase (RNA) II (DNA directed) polypeptide D (Predicted)	16	D4A259_RAT	-	21	32	0.61**	HD

* Control vs NGF ** NGF vs NGF+4-NP

Table 7.1 Alzheimer's Pathway affected proteins

	Protein Name	Accession Number	Log2 #	Spectral Count
CSK Control vs 4-NP	NADH dehydrogenase [ubiquinone] 1 alpha subcomplex subunit 2	D3ZS58_RAT	-3.36	2
	NADH dehydrogenase [ubiquinone] iron-sulfur protein 6	D3ZCZ9_RAT	-1.86	
	Cytochrome c oxidase subunit 6C-2	CX6C2_RAT	0.406	32
	Cytochrome c oxidase subunit 5A, mitochondrial	COX5A_RAT	0.465	145
	NADH:ubiquinone oxidoreductase subunit B10 SV=1	D4A0T0_RAT	0.551	23
	Cytochrome c oxidase subunit 2	COX2_RAT	0.65	36
	Succinate dehydrogenase [ubiquinone] iron-sulfur subunit	SDHB_RAT	0.898	36
	Succinate dehydrogenase [ubiquinone] flavoprotein subunit	SDHA_RAT	0.985	86
	Cytochrome c oxidase subunit 4 isoform 2	COX42_RAT	2.05	
	NADH dehydrogenase [ubiquinone] 1 beta subcomplex subunit 8	B2RYS8_RAT	2.05	10

CHAPTER 4: DISCUSSION

Because the U.S population is growing older, and aging is the most consistent risk factor of developing a neurodegenerative disorder, neurodegenerative diseases are expected to surge in the coming years. Since the pathogenesis of many of these diseases is unknown, the role of environmental factors must be considered. Until recently, the major concerns of environmental factors on human health were centered on potential roles in cancer. However, attention is now focused on understanding the damaging role of environmental factors on developing and mature nervous systems. Recent evidence suggests that environmental chemicals that act as endocrine disruptors (EDC) may adversely affect brain development and induce neurodegeneration. The results presented in this study demonstrate that 4-Nolylphenol (4-NP), an EDC, inhibits NGF-induced neuronal differentiation of PC12 cells by altering MT-Gβγ association. Dynamic rearrangement of microtubules (MTs) is critical for growth-cone motility and neurite outgrowth. Previously, Gβγ has been shown to play a key role in this process by stimulating MT assembly required for neurite outgrowth. This was further supported by the fact that blocking Gβγ-MT interaction by a Gβγ-sequestering peptide, GRK2i, inhibited neurite outgrowth and induced neurodegeneration (Sierra Fonseca et. al., 2014). The observation that 4-NP alters MT organization and its association with Gβγ suggests that 4-NP induces neurodegeneration by affecting the Gβγ-MT mediated pathway.

Proteomic analysis of cytoskeletal fraction (CSK) of 4-NP-treated PC12 cells (both control PC12 and NGF-differentiated cells) produced many interesting results. Because of the insoluble nature of CSK fraction, little attempt was made in the past to carry out proteomic analysis of this cellular structure. However, recently, while this study was in progress, a group of investigators

claimed to enrich CSK fraction from mouse embryonic fibroblasts for proteomic analysis (Choi et.al., 2013; Klemke et. al., 2013). Although this analysis indicated that actin cytoskeleton and focal adhesion-associated proteins were preserved in CSK preparation, microtubule cytoskeleton was disrupted during the purification steps used by these investigators. Our result indicates that MTs and other cytoskeletal proteins were preserved in CSK fraction isolated using our protocol. In addition, heterotrimeric G protein subunits were found to be associated with cytoskeletal fractions. This finding supports the core hypothesis of our laboratory research—that Gβγ is an integral component of cell cytoskeleton. The result also suggests that NGF-induced neuronal differentiation involves up- or down-regulation of these proteins.

We found that all tubulin, actin, and microtubule-associated protein isotypes, were significantly upregulated in the presence NGF in CSK. Among the tubulin isotypes, Tubulin beta 3 isotype (neuron-specific protein) was slightly up-regulated in the presence of 4-NP, while beta chain was slightly down-regulated (Table 1.1). Regarding G protein subunits, Gβ1 and Gβ2 were consistently associated with CSK fractions in PC12 cells (control and NGF-differentiated) and significantly up-regulated in the presence 4-NP (Table 1.1). This is an interesting observation. Although Gβγ association with MTs was shown to be important for MT assembly, and overexpression of Gβγ promotes neurite outgrowth (Sierra-Fonseca 2014, 2017), 4-NP was shown to inhibit neurite outgrowth, induce cellular degeneration and damage in NGF differentiated and Gβγ-overexpressed cells. Thus, it appears that adequate expression level of Gβγ is critical for neuronal differentiation and morphology. In fact, although overexpression of Gβγ induced neuronal differentiation, many of the Gβγ overexpressed cells had altered morphology (Sierra-Fonseca et.al 2014). Therefore, it is likely that upregulation of Gβ observed in the presence of 4-

NP might have played an important role in cytoskeletal disruption and neuronal damage observed in 4-NP-exposed cells.

We found that most of the tubulin isotypes that were up-regulated in CSK in response to NGF were also increased in WCL (Table 2.1). However, unlike CSK where several MAPs were up-regulated, only MAP1B was upregulated in WCL. Most surprisingly, all G protein subunits were significantly down-regulated in the presence NGF in WCL, and unlike CSK fractions, 4-NP did not have any significant effects on the expression of these proteins in WCL. Only protein that was affected by 4-NP was MAP4. Several genes, CBR1, MAP1a, Huntington Interacting protein 1, are apparent in several neurodegenerative diseases, such as Alzheimer's disease, Huntington's, and Parkinson's disease. Interestingly, these genes are affected after NGF and/or after 4-NP treatment.

String Link and gene ontology (GO) enrichment analysis indicated that many proteins in AD, PD, and HD pathways were affected by NGF (Table 6.1). While many of these proteins were downregulated in the presence of NGF, they were significantly upregulated after treatment with 4-NP. The results clearly suggest that 4-NP inhibits neuronal differentiation, and promotes neurodegenerative processes by upregulating the proteins involved in AD, PD and HD pathways. Future experiments will be designed to understand the role of these proteins in CSK disruption and neurodegeneration.

In summary, I have demonstrated that 4-NP at concentrations (5-10µM, ~1000-2000µg/L) was potent in inducing cellular aggregation and neurodegeneration. Previous studies indicated that 4-NP at a concentration as low as 0.2µM (44.07 µg/L) affected neurite outgrowth (Martinez, UTEP MS thesis 2013). Most NP-effect is associated with water concentration ranging from 1 to 1000µg/L (California Environmental Protection Agency, 2009).

Concentrations of 4-nonylphenol in surface waters are in the range of 0.11 to 180 µg/L (Tanghe and Verstraete, 2001). However, this concentration may not reflect 4-NP exposure in the environment, based on 4-NP's low solubility and hydrophobicity, and higher concentrations often detected in Biosolid and sediment samples. Using PC12 cells as a model system, our study clearly demonstrates the potential risk of 4-NP in affecting neuronal development and inducing neurodegeneration, and should provide essential information in accessing environment risk of 4-NP.

REFERENCES

Alonso, A.C., Li, B., Grundke-Iqbal, I., Iqbal, K. (2008). Mechanism of tau-induced neurodegeneration in Alzheimer disease and related tauopathies. Curr. Alzheimer Res. 5, 375-384.

Amniai L., Barbier, P., Sillen, A., Wieruszeski, J.M., Peyrot, V., Lippens, G., and Landrieu, I. (2008). Alzheimer disease specific phosphoepitopes of Tau interfere with assembly of tubulin but not binding to microtubules. *FASEB J.* 23, 1146–11452.

Arnold S. (2012) Cytochrome *c* Oxidase and Its Role in Neurodegeneration and Neuroprotection. In: Kadenbach B. (eds) Mitochondrial Oxidative Phosphorylation. Advances in Experimental Medicine and Biology, vol 748. Springer, New York, NY

Bevan, C.L., Porter, D.M., Schumann, C.R., Bryleva, E.Y., Hendershot, T.J., Liu, H., Howard, M.J., Henderson, L.P. (2006). The endocrine-disrupting compound, nonylphenol, inhibits neurotrophin-dependent neurite outgrowth. Endocrinology. 147, 4192-204.

California Environmental Protection Agency. Office of Environmental Health Hazard Assessment. 2009. Toxicological profile for nolylphenol

Cantley, L.C. (2002). The phosphoinositide 3-kinase pathway. Science. 296, 1655-1657.

Clemmensen, C., Aznar, S., Knudsen, G.M. et al. Cell Mol Neurobiol (2012) 32: 561. https://doi.org/10.1007/s10571-011-9796-9

Geraldo, S., Gordon-Weeks, P. R. 2009. Cytoskeletal dynamics in growth-cone steering. *J. Cell. Sci*. 122, 3595–3604.

Graves, P. R., & Haystead, T. A. J. (2002). Molecular Biologist's Guide to Proteomics. Microbiology and Molecular Biology Reviews, 66(1), 39–63. http://doi.org/10.1128/MMBR.66.1.39-63.2002

Greene, L.A. and Tischler, A.S. (1976). Establishment of a noradrenergic clonal line of rat adrenal pheochromocytoma cells which respond to nerve growth factor. Proc. Natl. Acad. Sci. **73**, 2424-2428.

Gustav-Rothenberg, K., Lerner, A., Bonda, D.J., Lee, H.G., Zhu, X., Perry, G., Smith, M.A. (2010). Biomarkers in Alzheimer's disease: past, present and future. Biomark Med. 4, 15–26.

Knight, Z.A. (2010). Small molecule inhibitors of the PI3-kinase family. Curr. Top. Microbiol. Immunol. 347, 263-278.

Kudo, C., Wada, K., Masuda, T., Yonemura, T., Shibuya, A., Fujimoto, Y., et al. 2004. Nonylphenol induces the death of neural stem cells due to activation of the caspase cascade and regulation of the cell cycle. J Neurochemistry 88,1416–23.

Lehmann, D.M., Seneviratne, A.M., Smrcka, A.V. (2008). Small molecule disruption of G protein beta gamma subunit signaling inhibits neutrophil chemotaxis and inflammation. Mol. Pharmacol. 73, 410-418.

Martinez Jurado, Jessica. Endocrine disrupting compound 4-Nolylphenol and neurodegeneration. Master thesis. Biological sciences, UTEP 2013.

Montoya, V., Gutierrez, C., Najera, O., Leony, D., Varela-Ramirez, A., Popova, J., Rasenick, M. M., Das, S., Roychowdhury, S. (2007). G protein betagamma subunits interact with alphabeta- and gamma-tubulin and play a role in microtubule assembly in PC12 cells. Cell Motil. Cytoskeleton. *64*, 936–950.

Rashid, M. A., Haque, M., Akbar, M. (2016). Detoxification of Carbonyl Compounds by Carbonyl Reductase in Neurodegeneration. Advances in Neurobiology, 12, 355-65. doi: 10.1007/978-3-319-28383-8_19.

Roychowdhury, S., Rasenick, M. M. 1997. G protein beta1gamma2 subunits promote microtubule assembly. *J. Biol. Chem.* 272, 31476–31581.

Sierra-Fonseca, J.A, Najera, O., Martinez-Jurado, J., Walker, E.M., Varela-Ramirez, A., Khan, A.M., Miranda, M., Lamango, N.S., and Roychowdhury, S. (2014). BMC Neuroscience 15: 132 doi: 10.1186/s12868-014-0132-4.

Stephens, L.R., Eguinoa, A., Erdjument-Bromage, H., Lui, M., Cooke, F., Coadwell, J., Smrcka, A. S., Thelen, M., Cadwallader, K., Tempst, P., Hawkins, P.T. (1997). The G beta gamma sensitivity of a PI3K is dependent upon a tightly associated adaptor, p101. Cell. 89, 105-114.

U.S. Environmental Agency (2010). Overview Nonylphenol (NP) and Nonylphenol Ethoxylates (NPEs) Action Plan [RIN 2070-ZA09].

Wang, K., Wong, Y.H. (2009). G protein signaling controls the differentiation of multiple cell lineages. Biofactors. *35*, 232-238.

Wang, X., Huang, T., Bu, G., and Xu, H. (2014). Dysregulation of protein trafficking in neurodegeneration. Molecular Neurodegeneration. *9*, 31. doi: 10.1186/1750-1326-9-31

Witte, H., Bradke, F. (2008). The role of the cytoskeleton during neuronal polarization. *Curr. Opin. Neurobiol.* 18, 479–487.

Wu, E.H., Wong, Y.H. (2005). Pertussis toxin-sensitive Gi/o proteins are involved in nerve growth factor-induced pro-survival AKT signaling cascade in PC12 cells. Cell Signal. *17*, 881-890.

Xu, Jie, Yang, Wang, Jie, Yu, Hisham Hisham, Jamal, Liu, Xiao-Yun, Fan, Qi-Yuan and Yan, Li. (2010). Toxic Effect of Gestational Exposure to Nonylphenol on F1 Male Rats. 3United Nations University-International Institute for Global Health. Birth Defects Research (Part B) 89:418–428

Yoshikawa Y. (2005). Experimental behavioral tests using monkey and rat offspring born from mothers exposed perinatally to EDCs. Psychopharmacol 25:115–124.

Zhou, F.Q., Zhou, J., Dedhar, S., Wu, Y.H., Snider, W.D. (2004). NGF-induced axon growth is mediated by localized inactivation of GSK-3beta and functions of the microtubule plus end binding protein APC. Neuron. 42, 897-912.

CURRICULUM VITA

Cynthia Carreon was born in El Paso, TX in the year 1992. She graduated from Irvin High School and in the fall of 2010 entered Houston Baptist University. After her freshman year she transferred to The University of Texas at El Paso. While pursuing her bachelor's degree, she worked in the COURI program for several semesters. After she received her Bachelors of Science from The University of Texas at El Paso in 2015, she was accepted into the Graduate program of the Biology department at The University of Texas at El Paso. There she worked as a teaching assistant for General Biology, and Vertebrae Physiology. She also gave an oral presentation at the 3rd BBRC Symposium Health Disparities: From Molecules to Disease on September of 2017.

Contact Information: ccarreon2@miners.utep.edu

This thesis was typed by Cynthia Carreon.